POLISH POLAR RESEARCH
vol. 34, no. 2, pp. 169–200, 2013 doi: 10.2478/popore-2013-0012

Benthic foraminifera from Pine Island and Ferrero bays, Amundsen Sea

Wojciech MAJEWSKI

Instytut Paleobiologii PAN, ul. Twarda 51/55, 00-818 Warszawa, Poland
<wmaj@twarda.pan.pl>

Abstract: Twenty one core tops from the central part of Pine Island Bay and nearby Ferrero Bay were collected in early 2010. They originate from a poorly studied area of the Amundsen Sea influenced at greater depths by relatively warm Circumpolar Deep Water. Almost all samples came from water-depths between 550 and 900 m and yield benthic foraminiferal assemblages of moderate variability with a significant decrease in calcareous forms with increasing water-depth. In total, 93 benthic taxa, belonging to 71 genera, are identified at the species level. They share a greater percentage of common species with the Ross Sea than with South Shetland Islands, most likely due to stronger climatic dissimilarity with the latter. Interestingly, the assemblages from Pine Island Bay, share the greatest numbers of taxa with assemblages described from Lützow-Holm Bay in East Antarctica, where the influence of Circumpolar Deep Water has been also recognized.

Key words: West Antarctica, Pine Island Bay, faunal gradient, dissolution, Circumpolar Deep Water.

Introduction

Although the area of the Pine Island and Ferrero bays, a part of the Amundsen Sea Embayment, is heavily glaciated, it is among the most unstable environments within the entire Antarctic continent. The reason for this instability is that relatively warm (~ 1°C) Circumpolar Deep Water (CDW), present at greater water depths, strongly affects local ice shelves and glaciers (Jacobs *et al.* 2011, 2012). The history of CDW influence on the Pine Island Bay (PIB) environment dates back at least several thousand years. The outer PIB was covered by a floating ice shelf between 12.3 and 10.6 thousand years ago. The subsequent rapid disintegration of this ice shelf was attributed to a widespread impingement of the CDW onto the continental shelf (Kirshner *et al.* 2012). Moreover, at present, CDW is channeled through a submarine trough and penetrates deep into the PIB, affecting tide water glaciers and ice shelves (Walker *et al.* 2007; Thoma *et al.* 2008). During the

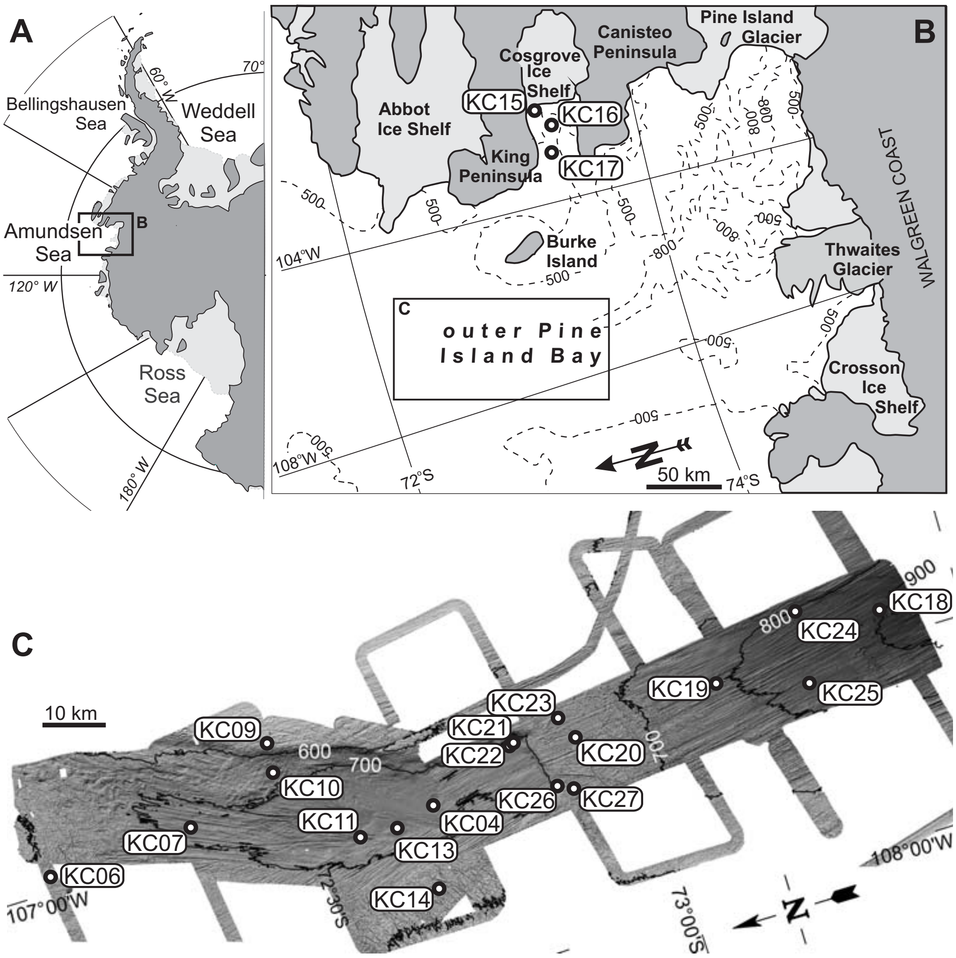

Fig. 1. Location of the study area, showing (**A**) West Antarctica, (**B**) Pine Island Bay sector of the Amundsen Sea Embayment with geographic nomenclature after Nitsche *et al.* (2007), and (**C**) the bathymetry of outer Pine Island Bay after Jakobsson *et al.* (2011). Note inset of C marked on B and sampling stations indicated by circles on maps B and C.

last decade, the volume and temperature of CDW has been increasing (Jacobs *et al.* 2011), while sea-ice has slightly decreased (Maksym *et al.* 2012).

The PIB area is fed by Coscrove Ice Shelf as well as by the Thwaites and Pine Island glaciers (Fig. 1). The latter is the third-largest drainage outlet for the West Antarctic Ice Sheet. It has experienced episodes of rapid disintegration since the Last Glacial Maximum (Lowe and Anderson 2002; Jakobsson *et al.* 2011), and remained dynamic during recent decades (Rignot *et al.* 2002). Pine Island Glacier together with the nearby Thwaites Glacier account for the most rapid recent regional loss of ice volume within Antarctica (Rignot *et al.* 2008), raising concerns about the stability of the entire West Antarctic Ice Sheet. The urge to better understand the history of local environmental changes is one of the reasons driving increasing research activities in this particular part of Amundsen Sea.

PIB is also one of the most remote areas of West Antarctica. It is located approximately half way between the Ross Sea and Antarctic Peninsula, two areas of intense scientific activity. PIB is in the center of the largest region of Antarctic shelf waters that remains poorly explored by biolgists (Griffiths 2010). Only few studies have addressed foraminifera. The works of Pflum (1966) and Kellogg and Kellogg (1987) concerned large areas from near-shore to outer shelf, including the Amundsen Sea, but because of sparse sampling they could address only general aspects of foraminiferal distribution and ecology. More detailed studies have been carried out around the Antarctic Peninsula and in the Bellingshausen Sea (Ishman and Domack 1994), where foraminiferal assemblages related to CDW and Weddell Sea Transitional Water were recognized, as well as in the South Shetland Islands (Finger and Lipps 1981; Mayer 2000; Majewski 2005, 2010; Majewski *et al.* 2007; Rodriguez *et al.* 2010). Numerous studies on foraminiferal distribution and ecology have been also carried on in the Ross Sea area (Fillon 1974; Osterman and Kellogg 1979; Bernhard 1987; Ward *et al.* 1987; Gooday *et al.* 1996; Violanti 1996).

The present study focuses on foraminiferal assemblages from core-tops collected in the central part of the outer PIB. These samples represent relatively narrow limits in terms of geographic distribution and bathymetry, having been collected mainly between 550 and 900 mwd (meters water depth) (Fig. 1, Table 1). Most of the samples came directly from the major trough within PIB that was penetrated recently by CDW. The main objective of this study is to explore the taxonomic composition of benthic foraminiferal assemblages in this poorly studied area influence by relatively warm CDW, and link them with assemblages from other regions of Antarctica.

Methods

Sampling and micropaleontological analysis. — Twenty two sediment cores were taken using Kasten corer during the *Oden* Southern Ocean 0910 (OSO0910) expedition in the austral summer of early 2010. Eighteen cores were taken from the central part of PIB (Fig. 1c) and three from the adjacent Ferrero Bay (Fig 1b). All samples, except for KC-15 taken at 1257 mwd, came from water depths between 548 and 894 m (Table 1). Because the sampling strategy was not designed for foraminiferal studies but for geological survey targeting late Quaternary sediments (Kirshner *et al.* 2012), it had some weaknesses. First of all, the site selection did not explore in full the variety of environments and bathymetries within the area. Moreover, using Kasten corer, which was intended to increase amount of sediment available for down-core analyses, was not ideal for preserving

Table 1

List of sampling stations with site locations and bathymetries.

Core ID	Longitude (°S)	Latitude (°W)	Water depth (m)
KC04	107.1105	72.6971	729
KC06	106.91	72.1325	612
KC07	106.8823	72.3394	707
KC09	106.3834	72.2920	548
KC10	106.4641	72.2954	687
KC11	107.911	72.3457	733
KC13	107.1687	72.6407	742
KC14	107.513	72.6503	639
KC15	101.8362	73.3603	1257
KC16	102.0792	73.4540	706
KC17	102.8267	73.4197	855
KC18	106.871	73.3835	894
KC19	106.9688	73.1285	782
KC20	107.0567	72.9102	671
tKC21	106.9563	72.8268	728
KC22	106.9633	72.8187	724
KC23	106.9243	72.8923	660
KC24	106.7568	73.2398	807
KC25	107.1057	73.2570	838
KC26	107.2223	72.8645	689
KC27	107.2548	72.8828	666

the sediment-water interface, inhabited by majority of living benthic foraminifera. Despite these limitations the upper-most 2 cm of sediment was sampled from each core for foraminiferal population studies.

The samples were wet-sieved with sea water through 63 μm sieve and stained with Rose Bengal (1 g per liter) in 70% ethanol diluted in sea water. The residues were washed in tap water and dried. At least 150 individuals were picked from each of the 63–125 μm and > 125 μm grain-size fractions. All samples, except KC-15, which yielded limited numbers of foraminifera, were divided using a dry microsplitter. Fractions of samples that have been picked for foraminifera were noted and are indicated in Appendices 1 and 2. Assemblage studies were performed under a light microscope, while a scanning electron microscope (SEM) was used for detailed taxonomic investigations. Foraminiferal specimens were arranged by taxa on micropaleontological slides. The classification scheme for the Order Foraminiferida used here is that of Loeblich and Tappan (1987). All taxa recognized are listed in Appendix 3 and SEM images are presented in Figs 2–11. The investigated material is housed at the Institute of Paleobiology of the Polish Academy of Sciences (Warszawa) under the catalogue number ZPAL F.65.

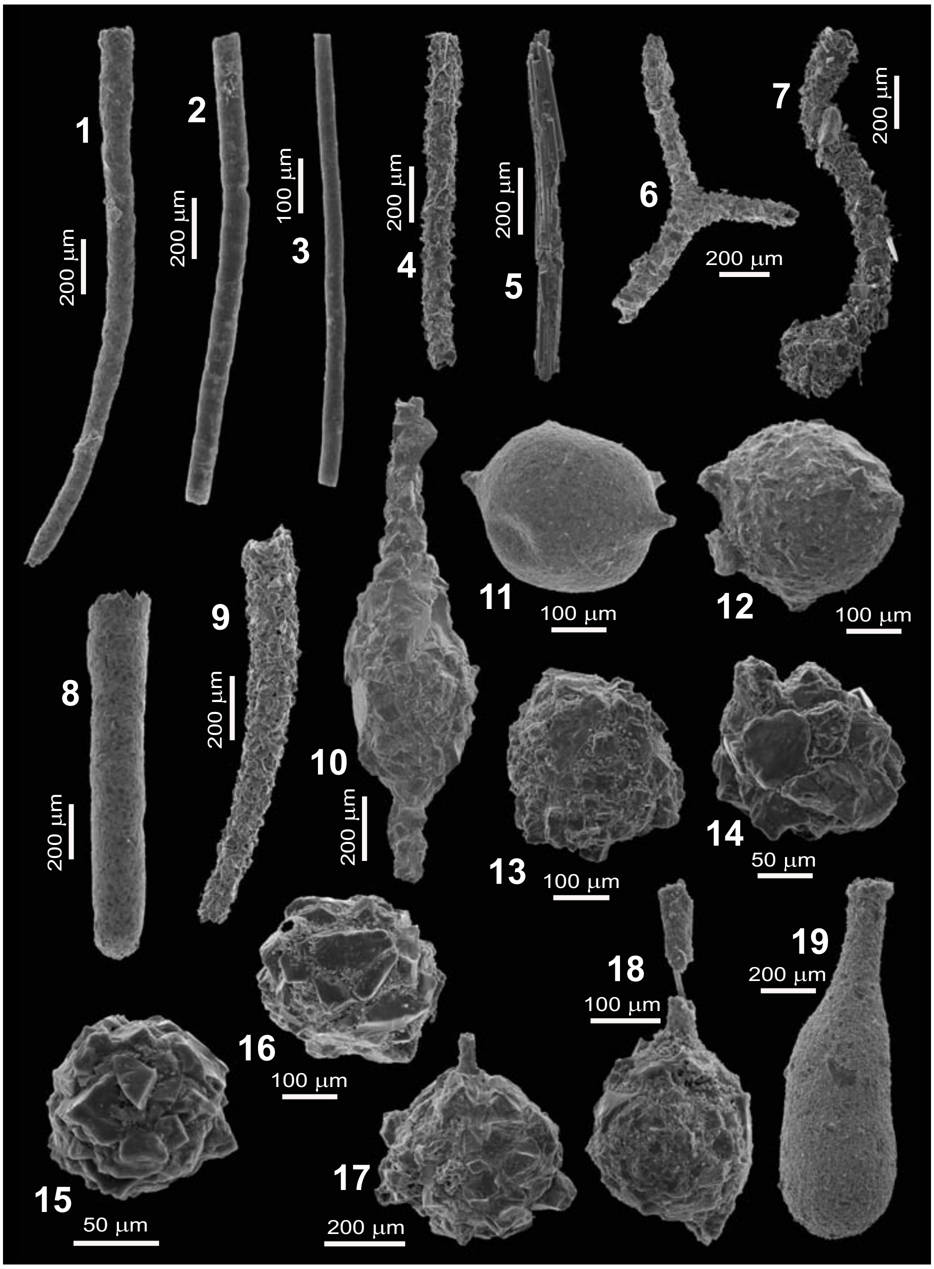

Fig. 2. SEM images of benthic foraminifera from Pine Island Bay. **1**–**2**. *Bathysiphon argenteus* Heron-Allen et Earland, 1913, KC04, KC11; **3**. *Bathysiphon flexilis* Höglund, 1947, KC15; **4**–**7**. *Rhabdammina* spp., KC11, KC23, KC04, KC04; **8**. ?*Hippocrepinella* sp., KC24; **9**. *Hyperammina fragilis* Höglund, 1947, KC19; **10**. *Pelosina bicaudata* (Parr, 1950), KC06; **11**. *Thurammina albicans* Brady, 1879, KC24; **12**. ?*Astrammina* sp., KC19; **13**. *Psammosphaera* sp. 1, KC24; **14**. *Psammosphaera* sp. 2, KC24; **15**. *Psammosphaera fusca* Schulze, 1875, KC15; **16**–**18**. *Saccammina tubulata* Rhumbler, 1931, KC21 (specimen with detached apertural tube), KC19, KC13; **19**. *Lagenammina* sp., KC18.

Table 2

Faunal parameters calculated for the total assemblages (> 63 μm dataset).

Core ID	Percent calcareous benthic foraminifera	Plankton-to-benthos ratio	Number of taxa	Shannon diversity index
KC04	64.4	0.027	39	2.02
KC06	71.8	0.274	34	2.40
KC07	66.5	0.204	39	2.33
KC09	87.7	0.363	34	2.05
KC10	99.0	0.374	26	1.47
KC11	34.8	0.036	36	2.65
KC13	35.6	0.067	35	2.55
KC14	22.4	0.029	36	2.81
KC15	12.7	0	33	3.11
KC16	8.6	0.006	32	2.80
KC17	4.8	0.011	34	2.94
KC18	18.4	0.034	29	2.82
KC19	14.6	0.010	35	2.72
KC20	12.1	0.008	32	2.84
KC21	59.3	0.096	31	2.22
KC22	63.6	0.150	37	2.48
KC23	14.1	0.005	30	2.82
KC24	8.0	0.025	33	2.78
KC25	26.9	0.023	28	2.64
KC26	46.7	0.110	37	2.54
KC27	54.5	0.142	36	2.67
Average	39.4	0.095	33.6	2.55
Standard deviation	28.6	0.117	3.45	0.38

Assemblage counts are listed in Appendices 1 and 2 separately for the 63–125 μm and > 125 μm fractions. Two datasets, from the coarse fraction (> 125 μm) as well as the > 63 μm fraction, *i.e.* combined data from the > 125 μm and 63–125 μm fractions were analyzed. For the latter combined dataset (the > 63 μm dataset), various assemblage parameters were calculated (Table 2). Faunal diversities are expressed as numbers of species identified in each sample, as well as Shannon diversity index $H = -\Sigma\, n_i/n \ln (n_i/n)$, where n_i is the number of individuals of species i. Plankton-to-benthos ratio is calculated as p/b ratio = $p/(p+b)$, where p indicates number of planktonic, and b number of benthic foraminifera.

Statistical analysis. — To improve understanding of the foraminiferal assemblages investigated in this study, the frequencies of foraminiferal species in the > 125 μm and > 63 μm datasets, were analyzed separately with orthogonal rotated (Varimax) principal component (PC) analysis, according to Malmgren and Haq

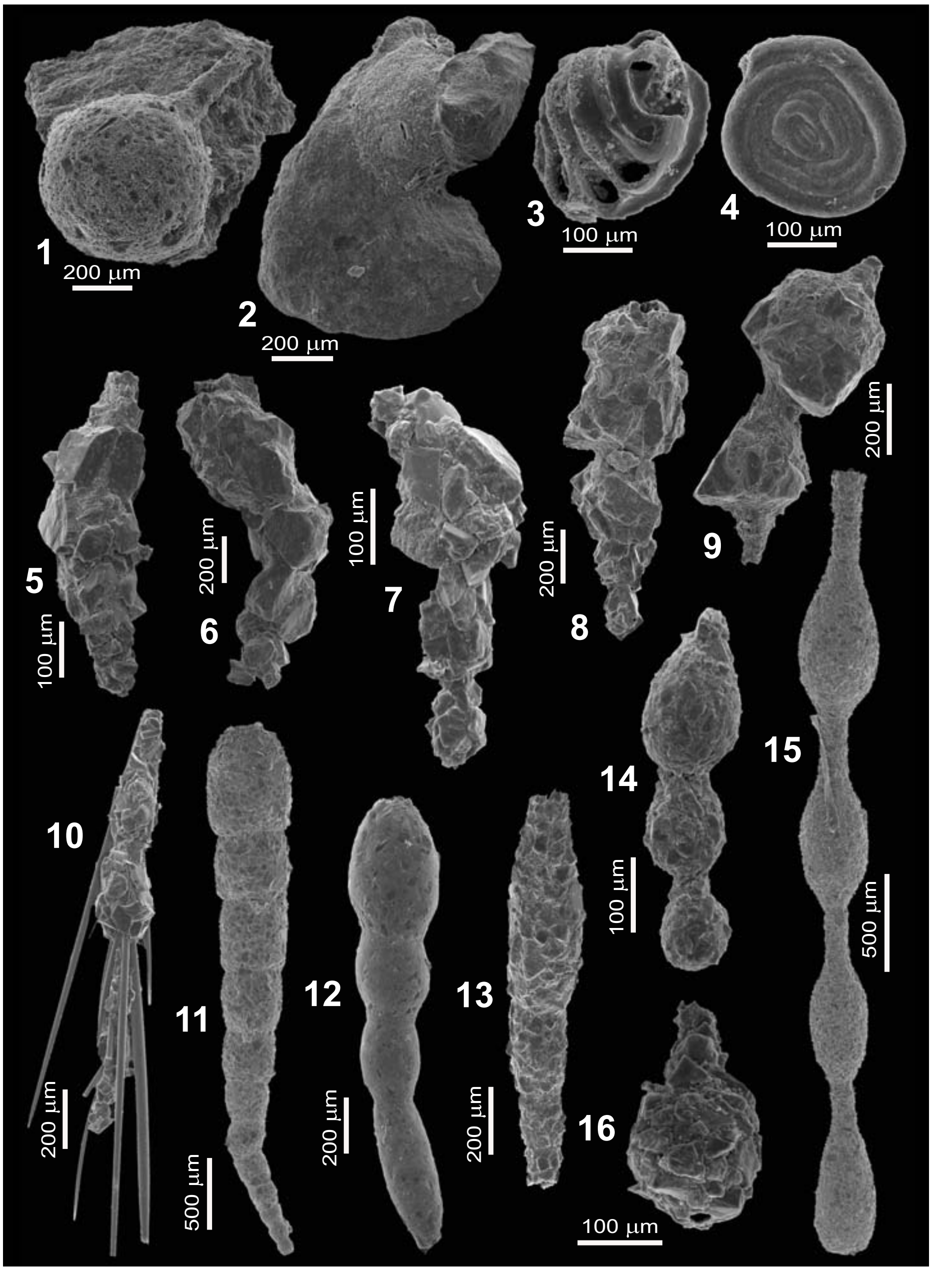

Fig. 3. SEM images of benthic foraminifera from Pine Island Bay. **1**. ?*Pseudothurammina* sp., KC11; **2**. *Tholosina* sp., KC26; **3**. *Glomospira gordialis* (Jones *et* Parker, 1860), KC23; **4**. *Ammodiscus incertus* (d'Orbigny, 1839), KC11; **5**. *Reophax subdentaliniformis* Parr, 1950, KC16; **6–8**. *Reophax scorpiurus* de Montfort, 1808, KC04, KC14, KC20; **9**. *Reophax* sp., KC25; **10**. *Reophax* cf. *R. spiculifer* Brady, 1879, KC04; **11**. *Pseudonodosinella nodulosa* (Brady, 1879), KC07; **12**. *Pseudonodosinella* cf. *P. nodulosa* (Brady, 1879), KC06; **13**. *Nodulina* cf. *N. dentaliniformis* (Brady, 1884), KC10; **14**. ?*Reophax* sp., KC17; **15–16**. *Hormosinella* spp., KC07, KC21.

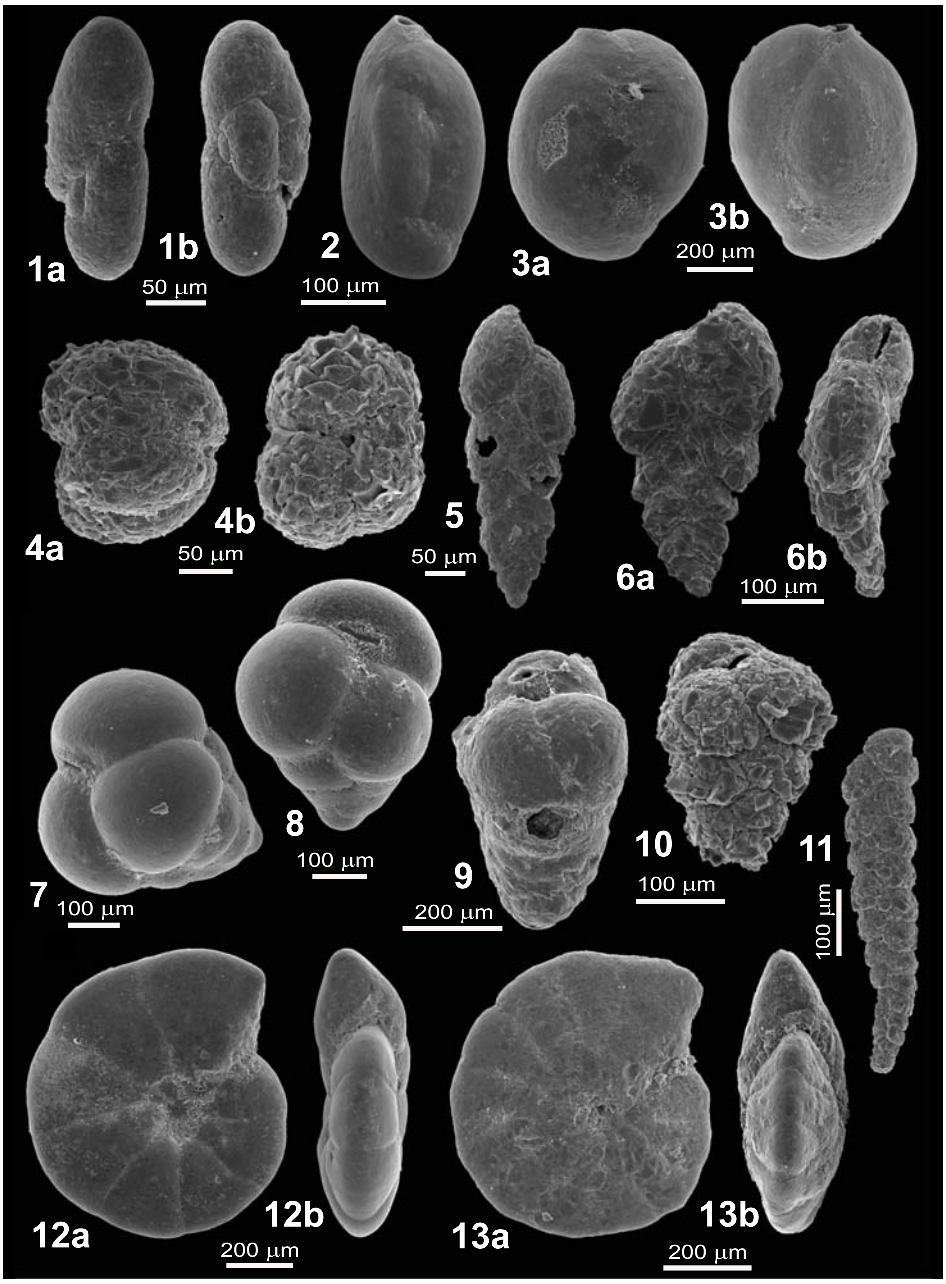

Fig. 4. SEM images of benthic foraminifera from Pine Island Bay. **1**. *Cystammina argentea* Earland, 1934, KC16; **2**. *Miliammina arenacea* (Chapman, 1916), KC14; **3**. *Miliammina lata* Heron-Allen *et* Earland, 1930, KC04; **4**. *Adercotryma glomerata* (Brady, 1878), KC11; **5–6**. *Pseudobolivina antarctica* Wiesner, 1931, KC11, KC16; **7–8**. *Eggerella nitens* (Wiesner, 1931), KC10, KC4; **9**. *Eggerella bradyi* (Cushman, 1911), KC18; **10**. *Verneuilina minuta* Wiesner, 1931, KC11; **11**. *Spiroplectammina biformis* (Parker *et* Jones, 1865), KC10; **12**. *Cyclammina trullissata* (Brady, 1879), KC04; **13**. *Cyclammina pusilla* Brady, 1884, KC04.

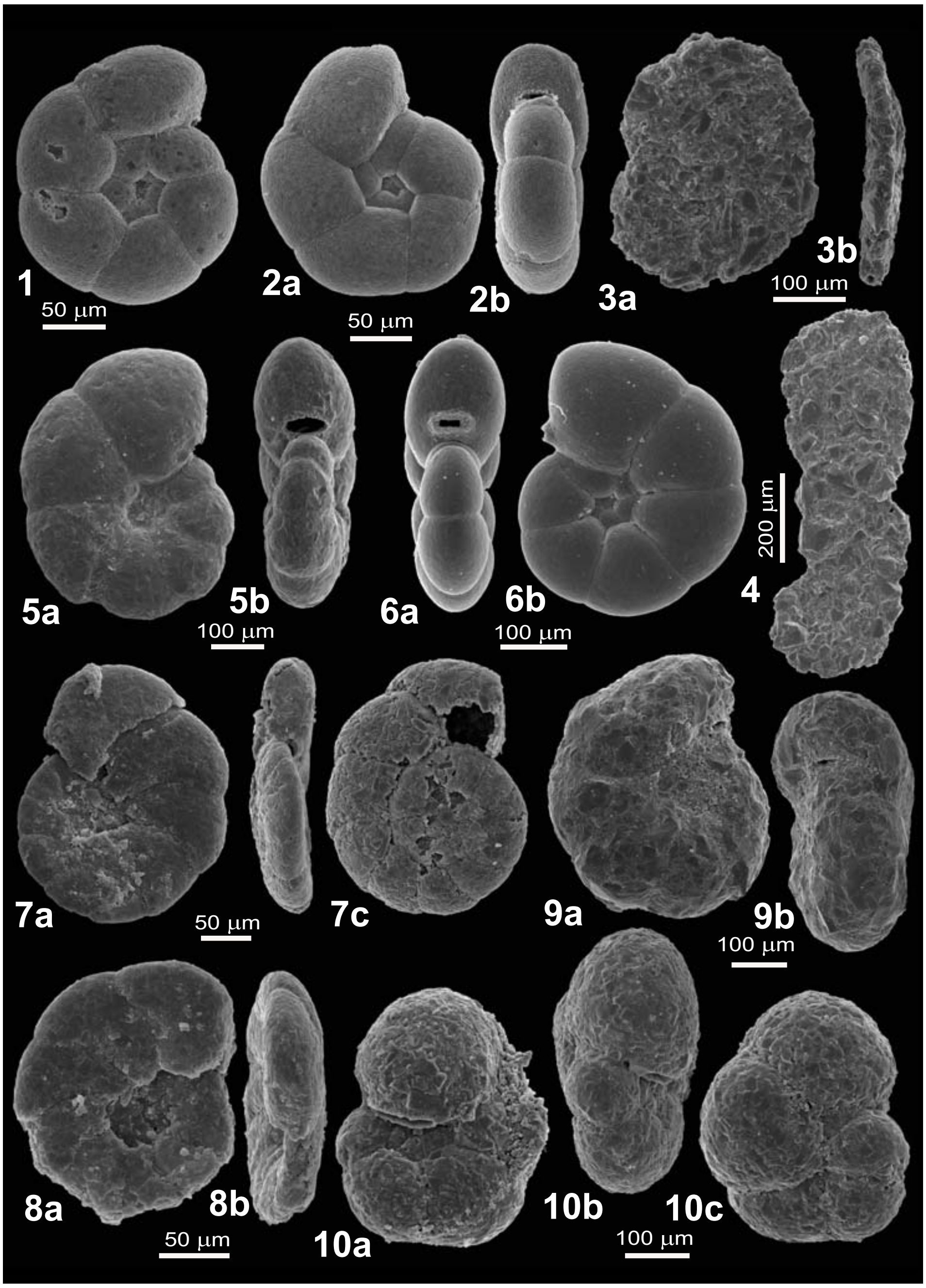

Fig. 5. SEM images of benthic foraminifera from Pine Island Bay. **1–2**. *Labrospira* sp., KC14, KC11; **3–4**. *Eratidus foliaceus* (Brady, 1881), KC18, KC04; **5**. *Labrospira jeffreysii* (Williamson, 1858), KC14; **6**. *Labrospira wiesneri* Parr, 1950, KC04; **7–8**. *Paratrochammina (Lepidoparatrochammina) lepida* Brönnimann *et* Whittaker, 1988, KC16, KC27; **9**. *Recurvoides contortus* Earland, 1934, KC16; **10**. *Atlantinella atlantica* (Parker, 1952), KC16.

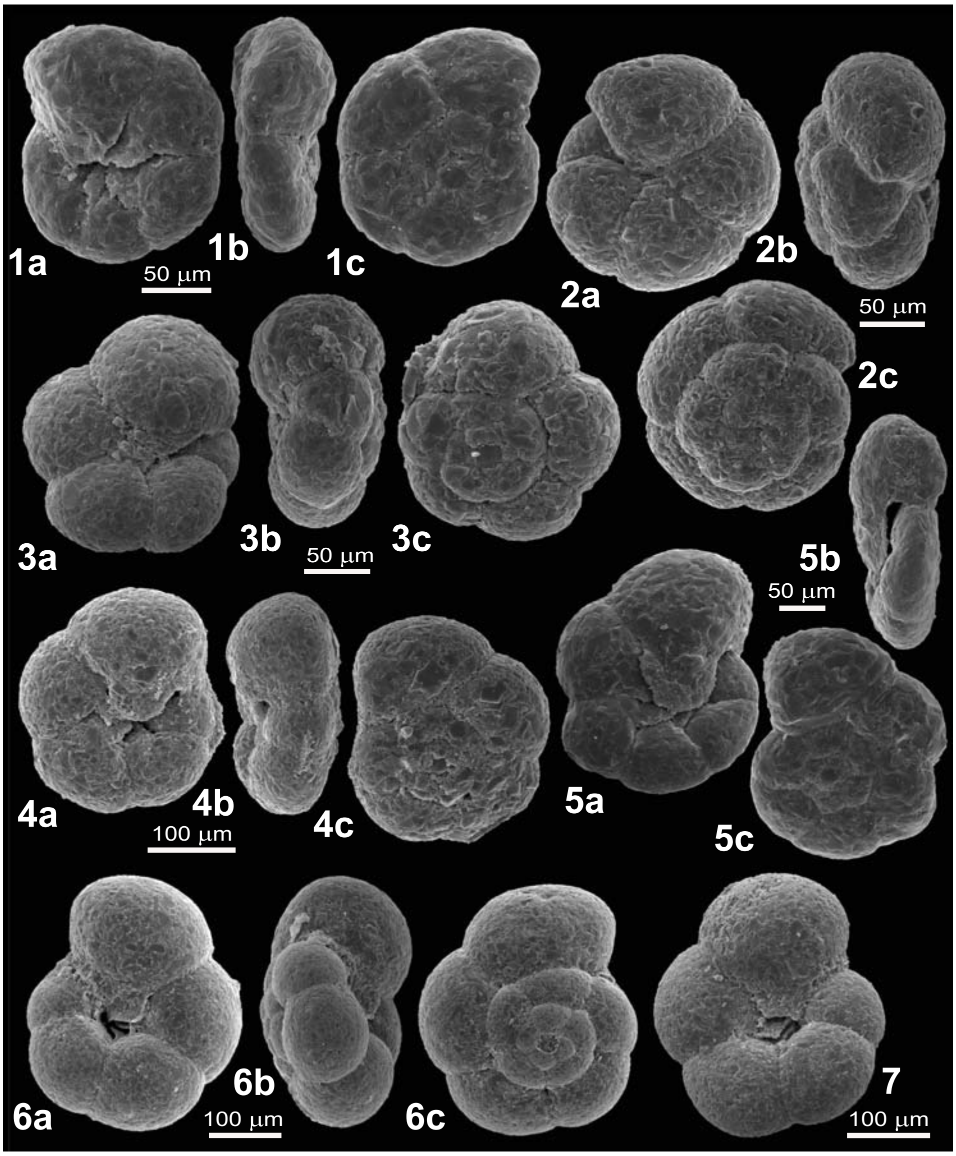

Fig. 6. SEM images of benthic foraminifera from Pine Island Bay. **1**. *Polystomammina falklandica* Brönnimann *et* Whittaker, 1988, KC15; **2**. *Portatrochammina* cf. *P. quadricamerata* (Echols, 1971), KC25; **3–4**. *Portatrochammina antarctica* Parr, 1950, KC14, KC20; **5**. *Portatrochammina bipolaris* Brönnimann *et* Whittaker, 1980, KC16; **6–7**. *Portatrochammina* cf. *P. antarctica* Parr, 1950, KC17, KC15.

(1982) and Mackensen *et al.* (1990). This procedure was chosen to reduce the number of variables to a manageable number without a significant loss of information. A commercially distributed statistics package (SYSTAT 12) was used. Only species that comprised more than 1% of the total fauna in at least three samples

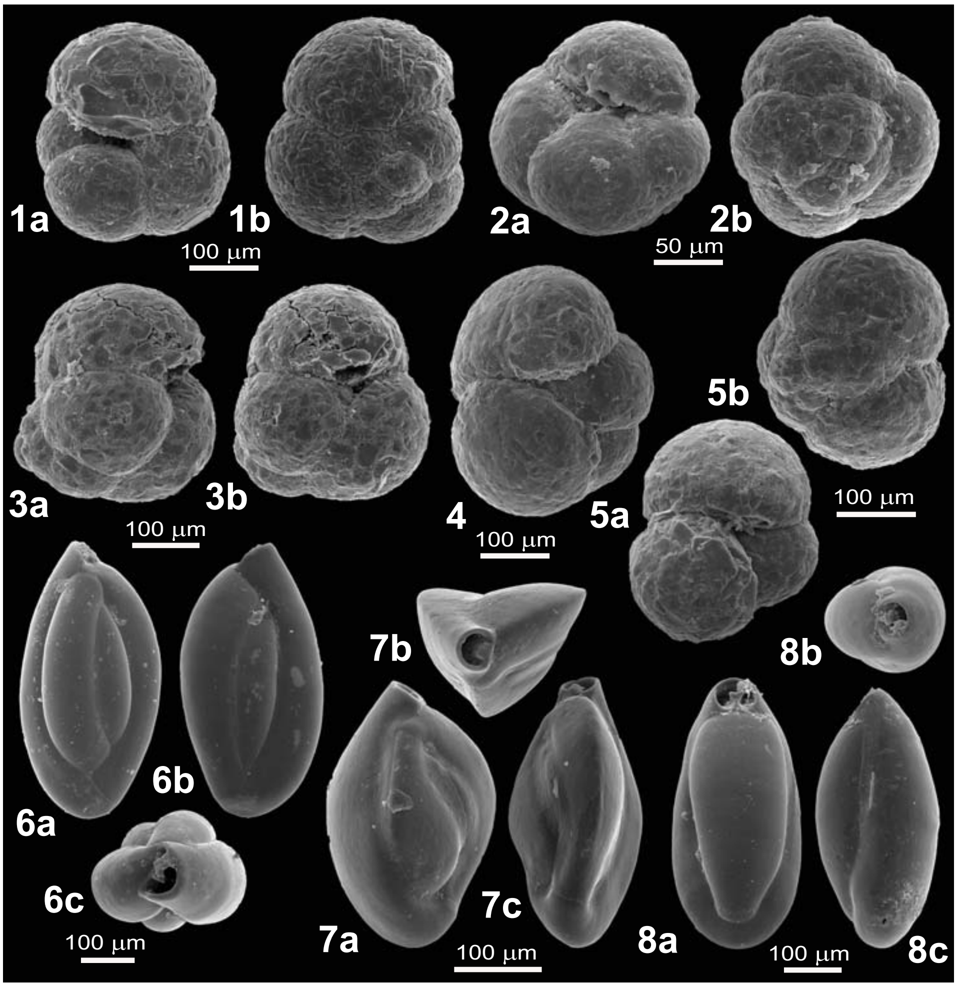

Fig. 7. SEM images of benthic foraminifera from Pine Island Bay. **1–2**. *Portatrochammina* spp., KC23, KC15; **2**. *Pseudotrochammina bullata* (Höglund 1947), KC04; **4–5**. *Alterammina alterans* (Earland, 1934), KC20, KC15; **6**. *Quinqueloculina* sp., KC04; **7**. *Triloculinella* sp., KC10; **8**. *Pyrgo elongata* (d'Orbigny, 1826), KC15.

were included in this statistical analysis. Two agglutinated genera, *Rhabdammina* and *Hormosinella*, were also excluded, as they easily disintegrate into multiple fragments, which could introduce a considerable bias into the dataset if counted as individuals. This procedure left 27 and 25 taxa for the > 125 μm and > 63 μm datasets, respectively.

The PC scores show the contribution of the selected variables (foraminiferal species) for each PC. Taxa that favor similar environmental conditions may have high scores on one PC, indicating their presence in one assemblage. PC loadings show similarities between assemblages from different sites. Those exceeding a

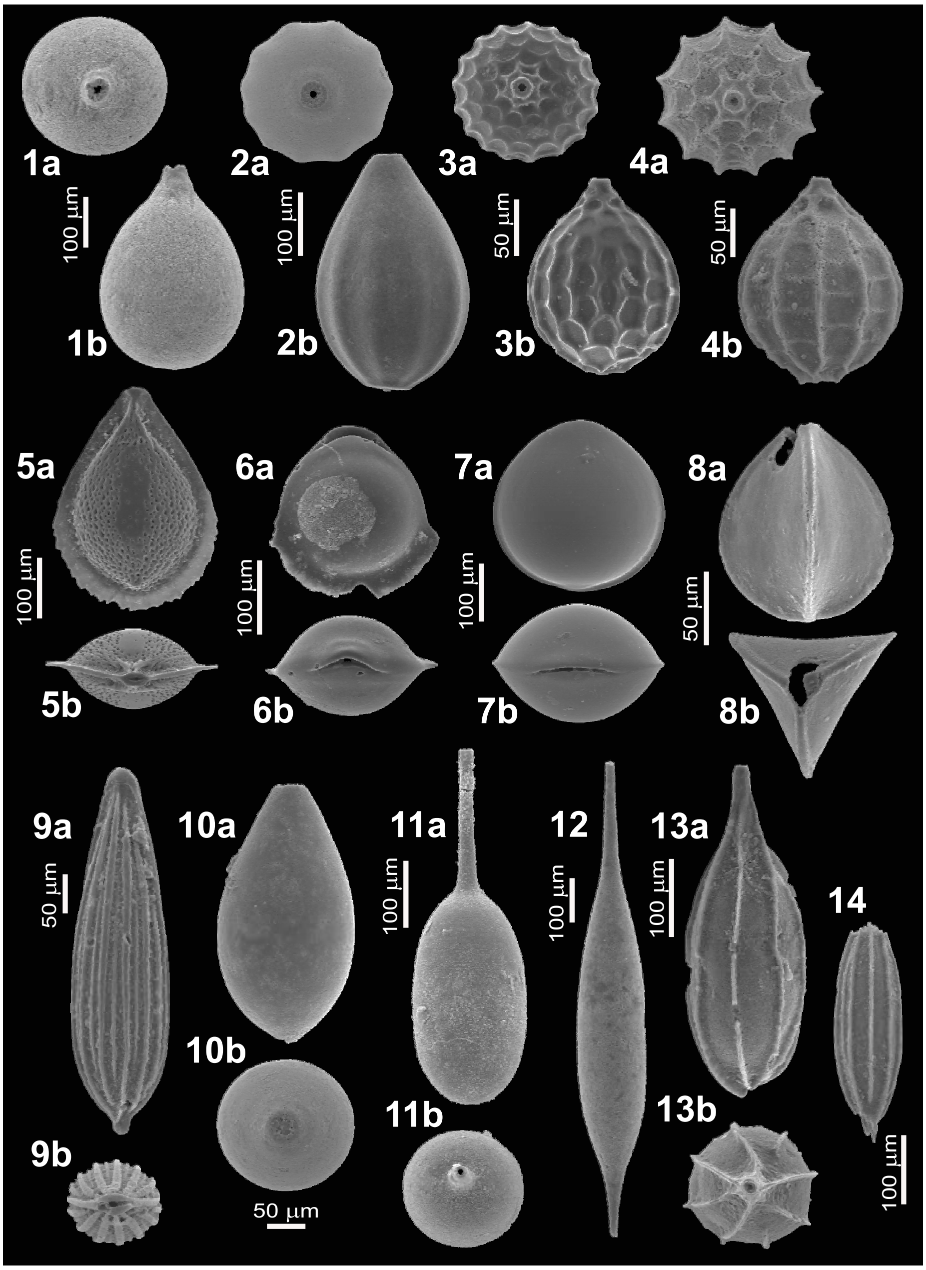

Fig. 8. SEM images of benthic foraminifera from Pine Island Bay. **1**. *Exsculptina* sp., KC06; **2**. *Lagena* sp., KC10; **3**. *Favulina hexagona* (Williamson, 1848), KC11; **4**. *Favulina scalariformis (*Williamson, 1848), KC10; **5.** *Lagena* cf. *L. texta* Wiesner, 1931, KC10; **6**. *Parafissurina* sp., KC06; **7**. *Parafissurina ventricosa* (Silvestri, 1904), KC10; **8**. *Galwayella trigonoeliptica* (Balkwill *et* Millett, 1884), KC09; **9**. ?*Vasicostella* sp., KC10; **10**. ?*Oolina* sp., KC10; **11**. *Pygmaeoseistron hispidulum* (Cushman, 1913), KC04; **12**. *Hyalinonetrion* sp. KC04; **13**. *Procerolagena meridionalis* (Wiesner, 1931), KC10; **14**. *Procerolagena gracilis* (Williamson, 1848), KC10 (fragmented specimen).

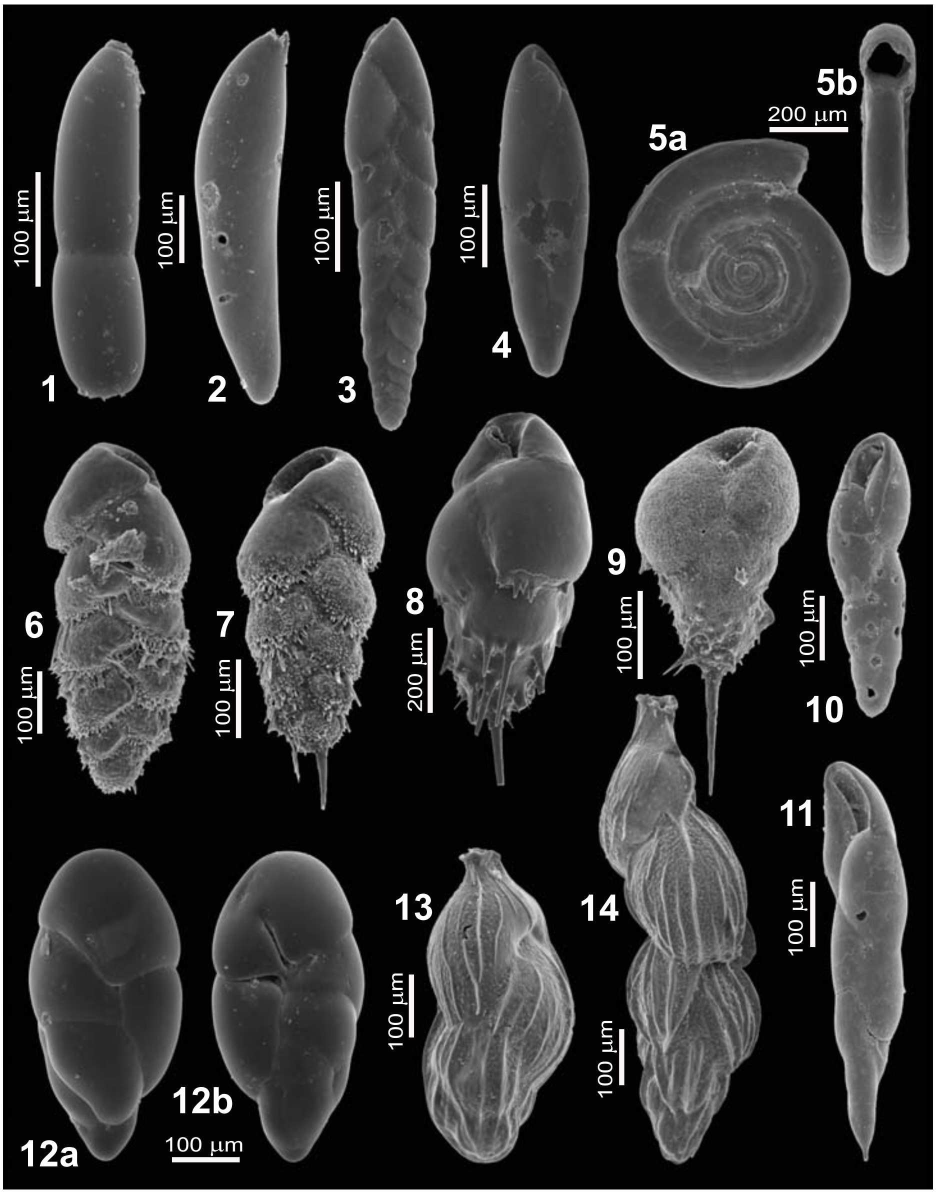

Fig. 9. SEM images of benthic foraminifera from Pine Island Bay. **1**. ?*Botuloides* sp., KC13; **2**. *Laevidentalina communis* (d'Orbigny, 1826), KC15; **3**. *Bolivinellina pseudopunctata* (Höglund, 1947), KC27; **4**. *Bolivinellina earlandi* (Parr, 1950), KC16; **5**. *Cornuspira involvens* (Reuss, 1850), KC10; **6–7**. *Bolivina* cf. *B. spinescens* Cushman, 1911, KC04, KC10; **8–9**. *Bulimina aculeata* d'Orbigny, 1826, KC10; KC09; **10–11**. *Stainforthia concava* (Höglund, 1947), KC04, KC06; **12**. *Robertinoides* sp., KC21; **13–14**. *Angulogerina earlandi* Parr, 1950, KC09, KC07.

value of 0.4 are regarded as statistically significant, following Malmgren and Haq (1982).

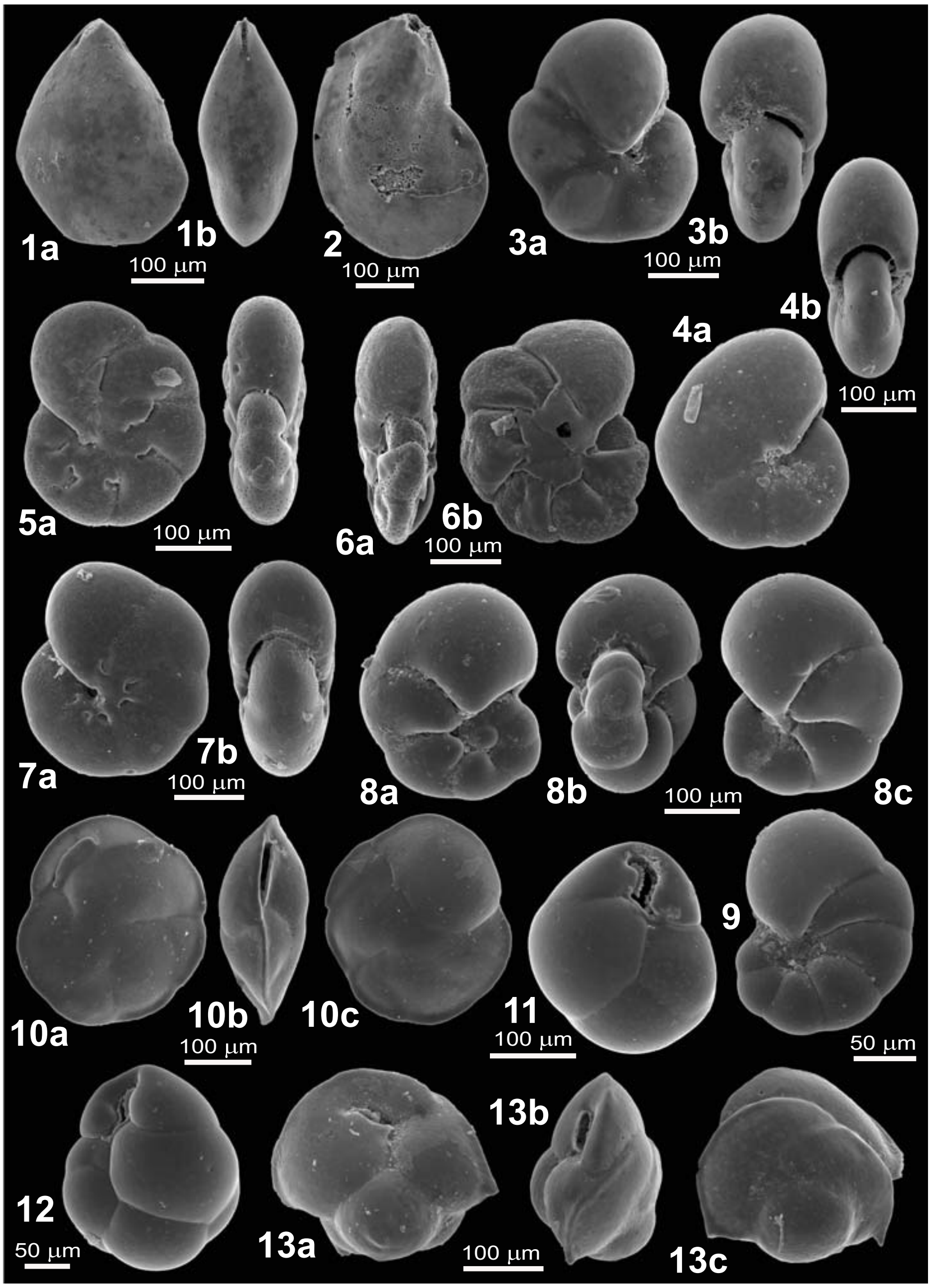

Fig. 10. SEM images of benthic foraminifera from Pine Island Bay. **1–2**. *Lenticulina angulata* (Reuss, 1851), KC10; KC06; **3–4**. *Pullenia salisburyi* Stewart *et* Stewart, 1930, KC17; KC04; **5–6**. *Astrononion antarcticum* Parr, 1950, KC09, KC06; **7**. *Astrononion echolsi* Kennet, 1967, KC10; **8–9**. *Nonionella iridea* Herron-Allen *et* Earland, 1932, KC09, KC10; **10**. *Cassidulina carinata* Silvestri, 1896, KC09; **11–12**. *Globocassidulina* spp., KC09, KC10; **13**. *Ehrenbergina glabra* Heron-Allen *et* Earland, 1922, KC10.

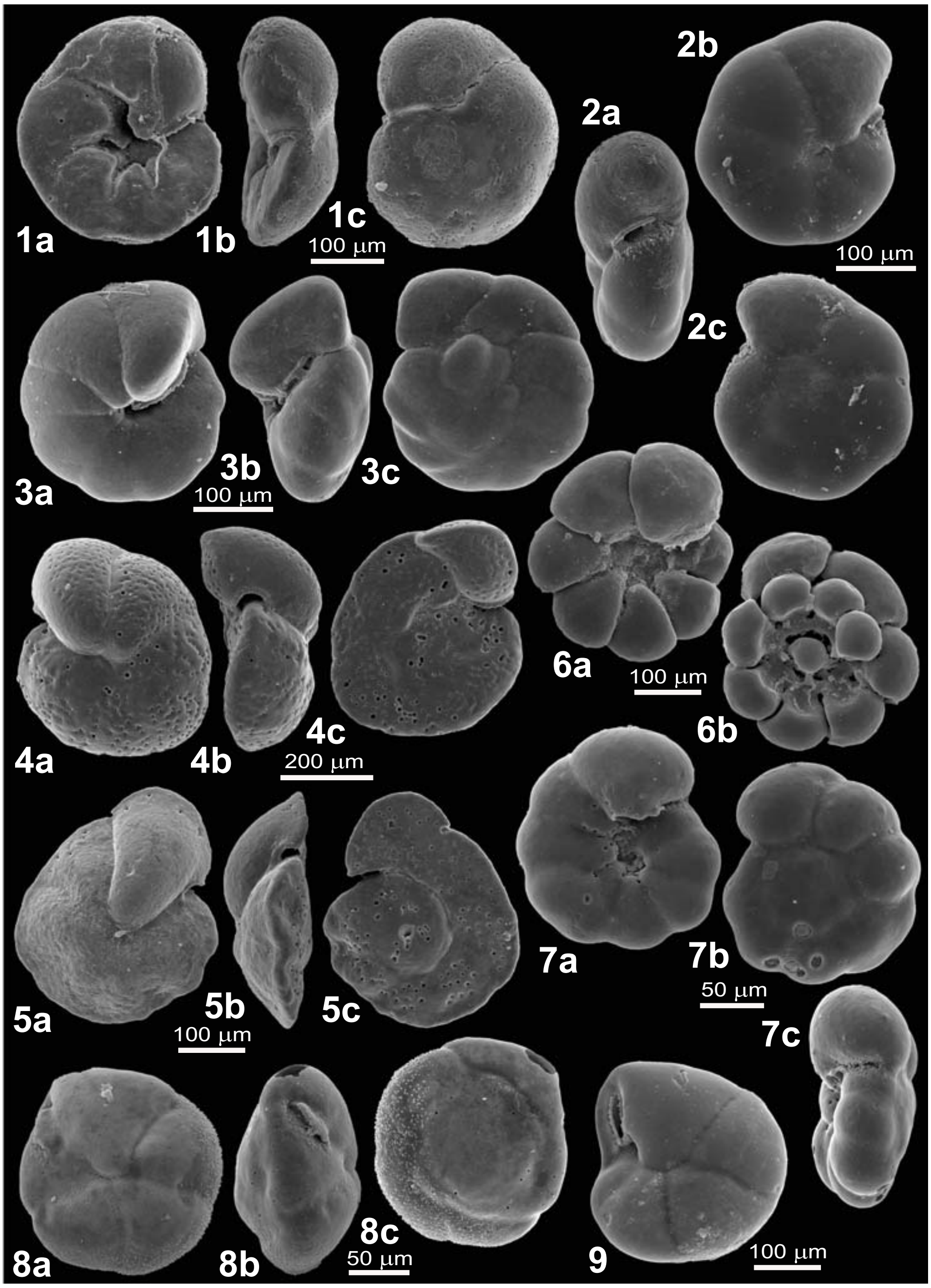

Fig. 11. SEM images of benthic foraminifera from Pine Island Bay. **1**. *Rosalina globularis* d'Orbigny, 1826, KC09; **2**. *Oridorsalis sidebottomi* (Earland, 1934), KC06; **3**. *Gyroidina* sp. KC09; **4**. *Cibicides refulgens* de Montfort, 1808, KC09; **5**. *Lobatula lobatula* (Walker *et* Jacob, 1798), KC09; **6–7**. *Ioanella tumidula* (Brady, 1884), KC19 (organic lining), KC06; **8–9**. *Epistominella* spp. (Brady, 1884), KC06, KC07.

Results

Census data. — A total of 6682 benthic foraminiferal specimens and 1992 planktonic specimens (*Neogloboquadrina pachyderma*) was recognized (Appendices 1 and 2), The benthic foraminifera represented 93 species, belonging to 71 genera (Appendix 3 and Figs 2–11). Very few individuals clearly stained with Rose Bengal were encountered. In addition, calcareous tests were in great majority opaque so they could by no means be part of living assemblages from the sediment-water interface. This absence of "living" benthic foraminiferal assemblage suggests missing upper-most portion of the cores.

The total assemblages (> 63 μm dataset) show moderate faunal variability (Table 2), with numbers of taxa in a single sample ranging from 26 to 39 (average 33.62) and Shannon diversity index between 1.5 and 3.1 (average 2.55); in both cases the standard deviations are an order of magnitude lower than the averages. More variability is exhibited among percentages of calcareous benthic foraminifera and plankton-to-benthos ratios, where averages and standard deviations are similar (Table 2). Assemblage composition is variable, although confined to a limited number of the most abundant taxa (Appendices 1 and 2), as discussed and interpreted in the following sections.

Results of the PC analysis. — For both the > 125 μm and > 63 μm datasets, three-PC models were selected in order to present changes between actual assemblages. They explain 85.4 and 94.5% of the total variance of the > 125 μm and > 63 μm datasets, respectively. The PCs are defined by variable numbers of foraminiferal species with large score values, noted in bold in Tables 3 and 4. The calculated PCs, which are mathematical models of actual assemblages, are referred to as foraminiferal assemblages (FA) throughout the following discussion.

For the larger fraction (the > 125 μm dataset), the most important FA accounting for 35.3% of the total variance of the dataset is defined by the strong presence of *Angulogerina earlandi*, together with accessory *Bulimina arenacea* (Table 3A). The second FA (29.1% of the total variance) is defined by a presence of *Portatrochammina* spp. together with *Milammina arenacea*, and the third FA (21.0%) by a strong presence of the single species *Alterammina alterans*.

For the total foraminiferal assemblages (the > 63 μm dataset) the most important FA, accounting for as much as 49.1% of the total variance, is defined by the strong presence of a single genus *Epistominella* spp. (Table 4A). The second FA (37.8% of the total variance) is defined by a strong presence of *Portatrochammina* spp. together with two accessory species *Adercotryma glomerata* and *Spiroplectammina biformis*. The third FA, accounting for only 7.6% of the total variance, is defined by strong presence of *Pseudobolivina antarctica* accompanied by *Adercotryma glomerata* and an absence of *Portatrochammina* spp.

Table 3

PC scores of the > 125 µm foraminiferal dataset from Pine Island and Ferrero bays, showing contribution of each of the 27 taxa (variables) to each assemblage (**A**) and PC loadings showing similarity between assemblages at different sites, arranged according to increasing water-depth (**B**). Statistically significant score and loading values are marked in bold.

A

Taxon	PC1	PC2	PC3
Hyperammina fragilis	-0.57	-0.34	-0.45
Psammosphaera spp.	-0.42	-0.24	-0.31
Reophax subdentaliniformis	-0.22	-0.3	-0.11
Reophax scorpiurus	-0.36	-0.04	-0.5
Reophax spiculifer	-0.12	0.24	0.21
Pseudonodosinella nodulosa	-0.5	-0.42	-0.32
Miliammina arenacea	-0.37	**1.36**	0.23
Adercotryma glomerata	0.03	0.6	0.39
Pseudobolivina antarctica	-0.3	-0.26	-0.46
Eggerella nitens	-0.43	-0.38	-0.51
Eggerella bradyi	-0.56	-0.29	-0.35
Spiroplectammina biformis	0.05	-0.25	0.31
Cyclammina pusilla	-0.23	-0.34	-0.11
Labrospira wiesneri	-0.45	-0.42	-0.4
Labrospira jeffreysii	-0.27	0.1	-0.7
Labrospira sp.	-0.61	-0.2	-0.41
Eratidus foliaceus	-0.54	0.32	0.25
Recurvoides contortus	-0.69	-0.3	0.24
***Portatrochammina* spp.**	0.38	**4.44**	-0.61
Alterammina alterans	-0.01	0.36	**4.57**
Bulimina aculeata	**2.05**	**-1.11**	0.52
Angulogerina earlandi	**4.16**	-0.01	-0.77
Astrononion echolsi	-0.52	-0.3	-0.53
Globocassidulina spp.	0.6	-0.71	0.83
Oridorsalis sidebottomi	-0.51	-0.51	-0.32
Ioanella tumidula	-0.09	-0.45	-0.52
Epistominella spp.	0.53	-0.54	-0.17

B

Water depth (m)	Core ID	PC1	PC2	PC3
548	KC09	**0.91**	0.04	-0.15
612	KC06	**0.94**	0.03	-0.05
639	KC14	**0.51**	**0.6**	0.42
660	KC23	0.47	**0.76**	-0.09
666	KC27	**0.95**	0.2	0.01
671	KC20	0.05	**0.66**	**0.62**
687	KC10	**0.97**	-0.15	-0.06
689	KC26	**0.81**	0.09	0.35
706	KC16	-0.02	**0.93**	-0.15
707	KC07	**0.65**	-0.18	**0.57**
724	KC22	**0.94**	0.18	0.15
728	KC21	**0.91**	0.27	-0.08
729	KC04	**0.74**	-0.03	0.48
733	KC11	0.14	0.36	**0.85**
742	KC13	0.12	0.27	**0.89**
782	KC19	0.03	**0.83**	0.4
807	KC24	0.02	**0.9**	0.35
838	KC25	-0.01	**0.71**	**0.66**
855	KC17	-0.01	**0.89**	0.25
894	KC18	0.09	**0.77**	0.29
1257	KC15	-0.15	0.19	**0.84**

Interpretation

Assemblage gradient with water-depth. — The results of the PC analyses show significant differences between the two datasets resulting from the distinctly taxonomic compositions in different grain-size fractions (Appendices 1 and 2). Despite these discrepancies, both analyses show similar patterns with the most important FAs (PC1s in both datasets) being defined by calcareous taxa and a number

Table 4

PC scores of the > 63 μm foraminiferal data set from Pine Island and Ferrero bays, showing contribution of each of the 25 taxa (variables) to each assemblage (**A**) and PC loadings showing similarity between assemblages at different sites, arranged according to increasing water-depth (**B**). Statistically significant score and loading values are marked in bold.

A

Taxon	PC1	PC2	PC3
Bathysiphon argenteus	-0.28	-0.56	-0.15
Reophax scorpiurus	-0.3	-0.53	-0.13
Reophax spiculifer	-0.29	-0.12	-0.46
Cystammina argentea	-0.32	-0.36	-0.06
Miliammina arenacea	-0.49	0.31	0.47
Adercotryma glomerata	-0.15	**1.15**	**2.45**
Pseudobolivina antarctica	-0.37	0.48	**3.59**
Spiroplectammina biformis	-0.1	**0.97**	0.01
Cyclammina pusilla	-0.31	-0.55	-0.08
Labrospira wiesneri	-0.32	-0.46	0.15
Labrospira jeffreysii	-0.28	-0.51	-0.14
Labrospira sp.	-0.3	-0.31	-0.54
Eratidus foliaceus	-0.35	-0.3	0.03
Paratrochammina lepida	-0.28	-0.3	-0.53
Recurvoides contortus	-0.28	-0.29	-0.63
Polystomammina falklandica	-0.32	-0.39	-0.33
***Portatrochammina* spp.**	-0.07	**4.2**	**-1.55**
Alterammina alterans	-0.21	0.57	-0.24
Bulimina aculeata	0.2	-0.6	-0.6
Angulogerina earlandi	0.31	-0.46	-0.67
Astrononion echolsi	-0.29	-0.51	-0.27
Nonionella iridea	-0.22	-0.53	-0.16
Globocassidulina spp.	0.1	-0.36	-0.2
Ioanella tumidula	0.23	-0.48	-0.23
***Epistominella* spp.**	**4.7**	-0.06	0.26

B

Water depth (m)	Core ID	PC1	PC2	PC3
548	KC09	**0.99**	-0.02	0.02
612	KC06	**0.93**	0.03	-0.03
639	KC14	0.4	**0.85**	0.2
660	KC23	0.25	**0.81**	0.42
666	KC27	**0.94**	0.29	0.05
671	KC20	0.11	**0.87**	0.31
687	KC10	**0.99**	-0.05	0.02
689	KC26	**0.91**	0.27	0.27
706	KC16	-0.05	**0.94**	0.04
707	KC07	**0.98**	0.04	0.08
724	KC22	**0.98**	0.15	0.11
728	KC21	**0.95**	0.23	0.18
729	KC04	**0.97**	0.16	0.11
733	KC11	**0.75**	0.37	**0.52**
742	KC13	**0.79**	0.37	0.46
782	KC19	0.2	**0.65**	**0.7**
807	KC24	0.07	**0.95**	0.19
838	KC25	**0.61**	**0.74**	0.13
855	KC17	-0.06	**0.96**	-0.12
894	KC18	0.35	**0.83**	0.3
1257	KC15	0.07	**0.94**	-0.08

of calcareous species showing positive PC scores for these particular FAs (Tables 3A and 4A). In contrast, the two less important FAs (PC2 and PC3) for each dataset are defined by agglutinated taxa, with most calcareous species showing negative PC scores. These results suggest that the strongest faunal differences between benthic foraminiferal FAs for each dataset are determined by test composition, *i.e.* dominated by calcareous *vs* agglutinated. The same relation is also supported by strong correlation between percentages of calcareous foraminifera and the most important FAs (*A. earlandi* FA and *Epistominella* spp. FA), indicated by correlation coefficient values of 0.87 and higher (Table 5).

Table 5

Linear correlation coefficients (*r*) calculated from the percentages of the most frequently occurring foraminiferal species (> 63 µm dataset), FAs, and faunal characteristics against bathymetric depths. The correlation coefficient approaches 1.0 and -1.0 as the positive and negative correlation increases. Correlation coefficients greater than 0.5 and lower than -0.5 are marked in bold.

				> 125 µm dataset			> 63 µm dataset		
	Water-depth	Percent calcareous benthics	Plankton-to-benthos ratio	*Angulogerina earlandi* FA	*Portatrochammina* spp. FA	*Alterammina alterans* FA	*Epistominella* spp. FA	*Portatrochammina* spp. FA	*Pseudobolivina antarctica* FA
Percent calcareous benthics	-0.47								
Plankton-to-benthos ratio	-0.47	**0.89**							
FAs for the > 125 µm dataset									
Angulogerina earlandi FA	**-0.61**	**0.87**	**0.74**						
Portatrochammina spp. FA	0.2	**-0.88**	**-0.72**	**-0.73**					
Alterammina alterans FA	**0.5**	-0.36	-0.48	**-0.57**	0.02				
FAs for the > 63 µm dataset									
Epistominella spp. FA	-0.47	**0.91**	**0.69**	**0.83**	**-0.85**	-0.14			
Portatrochammina spp. FA	**0.5**	**-0.96**	**-0.81**	**-0.84**	**0.88**	0.25	**-0.95**		
Pseudobolivina antarctica FA	-0.14	-0.32	-0.39	-0.28	0.32	0.34	-0.1	0.14	
The most frequently occurring foraminiferal species (> 63 µm dataset)									
Bathysiphon argenteus	-0.01	-0.12	-0.18	0.06	-0.02	0.2	0.02	0.06	0.22
Reophax scorpiurus	-0.24	-0.32	-0.22	-0.02	0.34	-0.2	-0.28	0.29	0.06
Reophax cf. *spiculifer*	**0.62**	**-0.64**	**-0.5**	**-0.63**	0.49	0.32	**-0.67**	**0.63**	-0.16
Cystammina argentea	**0.64**	**-0.68**	**-0.56**	**-0.73**	**0.53**	0.46	**-0.64**	**0.62**	0.26
Miliammina arenacea	0.32	**-0.73**	**-0.58**	**-0.69**	**0.75**	0.19	**-0.75**	**0.75**	0.37
Adercotryma glomerata	0.32	**-0.74**	**-0.82**	**-0.61**	**0.63**	0.45	-0.48	**0.57**	**0.76**
Pseudobolivina antarctica	-0.04	**-0.57**	**-0.6**	**-0.5**	**0.58**	0.3	-0.37	0.41	**0.88**
Spiroplectammina biformis	0.01	**-0.54**	**-0.59**	-0.2	0.36	0.08	-0.47	**0.53**	0.12
Cyclammina pusilla	-0.36	-0.02	0.03	0.1	-0.07	0.02	0.03	-0.08	0.23
Labrospira wiesneri	-0.26	-0.23	-0.33	-0.06	0.19	0.03	-0.17	0.2	0.25
Labrospira jeffreysii	-0.29	-0.12	-0.07	0.08	0.13	-0.4	-0.25	0.15	-0.2
Labrospira sp.	**0.6**	-0.44	-0.33	-0.5	0.26	0.05	**-0.58**	**0.51**	-0.39
Eratidus foliaceus	0.29	**-0.51**	-0.39	**-0.52**	**0.54**	0.23	-0.46	**0.53**	0.2
Paratrochammina lepida	0.05	-0.32	-0.11	-0.26	0.39	-0.39	**-0.51**	0.38	-0.4
Recurvoides contortus	**0.9**	-0.44	-0.34	**-0.54**	0.19	0.34	**-0.52**	**0.5**	-0.37
Polystomammina falklandica	0.32	**-0.5**	-0.36	-0.36	0.45	0.05	**-0.57**	**0.52**	-0.21
Portatrochammina spp.	0.41	**-0.84**	**-0.73**	**-0.72**	**0.84**	0.05	**-0.85**	**0.9**	-0.09
Alterammina alterans	**0.64**	**-0.64**	**-0.55**	**-0.75**	0.39	**0.77**	**-0.55**	**0.61**	0.13
Bulimina aculeata	-0.42	**0.84**	**0.83**	**0.82**	**-0.73**	-0.44	**0.73**	**-0.81**	-0.37
Angulogerina earlandi	-0.47	**0.61**	**0.72**	**0.65**	-0.45	**-0.54**	0.48	**-0.57**	-0.33
Astrononion echolsi	0.29	-0.16	0.02	-0.25	0.13	-0.23	-0.41	0.27	**-0.54**
Nonionella iridea	-0.24	**0.54**	**0.61**	0.41	-0.31	-0.28	0.46	-0.46	-0.14
Globocassidulina spp.	-0.18	**0.69**	**0.66**	**0.52**	**-0.69**	-0.05	**0.65**	**-0.65**	-0.29
Ioanella tumidula	**-0.61**	**0.9**	**0.76**	**0.88**	**-0.78**	-0.38	**0.82**	**-0.86**	-0.25
Epistominella spp.	-0.44	**0.97**	**0.8**	**0.82**	**-0.87**	-0.25	**0.93**	**-0.95**	-0.22

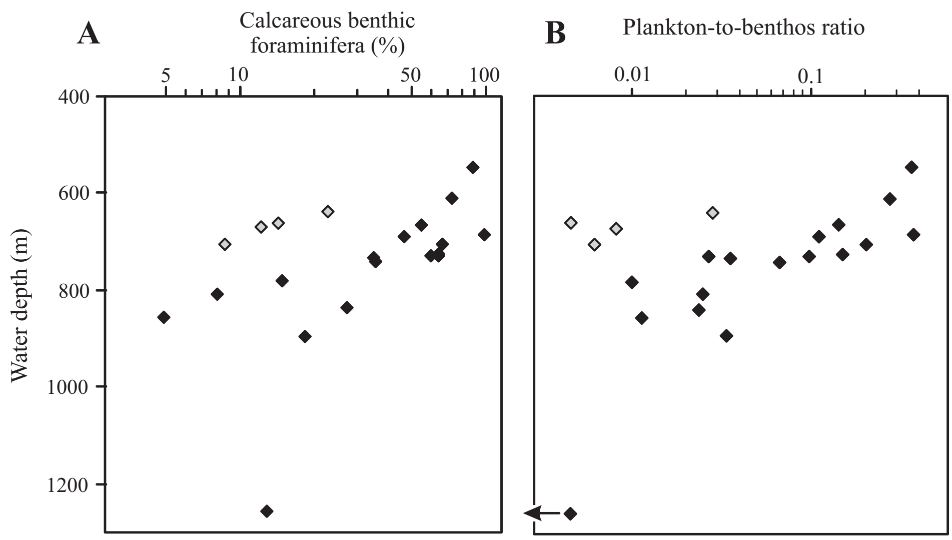

Fig. 12. Trends in percent of calcareous benthic foraminifera and plankton-to-benthos ratio, both in logarithmic scales, against water depth. Four odd samples KC14, KC16, KC20, and KC23 marked in gray.

It appears that, with some exceptions, assemblage composition and the faunal parameters are related to water-depth. When the FA scores are arranged according to increasing depth (Tables 3B and 4B), they show similar trend within each dataset, with the FAs defined by calcareous foraminifera dominating shallower-water setting. This trend is clear, despite the fact that four sites (KC14, KC16, KC20, and KC23) do not follow the pattern. The same four sites, marked in gray on Fig. 12, are also outside the general trends of decreasing percent calcareous foraminifera and plankton-to-benthos ratio with increasing water-depth.

The explanation for this inconsistency may lie in the non-synchronous age of the analyzed core tops. Firstly, the failure of the Rose Bengal staining, which is a conventional method to recognize presence of "living" foraminifera (*e.g.* Silva *et al.* 1996), suggests that the surficial sediment was lost during coring or core handling and the assemblages analyzed in this study were sub-fossil in character. Secondly, sites KC14, KC20, and KC23 are located in areas showing numerous iceberg plow marks (Jakobsson *et al.* 2011), which suggests the presence of disturbed near-surface sediments at these locations. Both mechanisms imply that, although consistently within the late Holocene (Kirshner *et al.* 2012), the precise age of the core tops investigated in this study is not known. It seems more than likely that it is rather variable. Thus age differences in combination with the dynamic environmental and micropaleontological record preserved in these cores (Kirshner *et al.* 2012), is probably responsible for obscuring the true relationship between foraminiferal assemblages and water-depth in Pine Island Bay.

Foraminiferal assemblages, dissolution, and different water masses. — There is also a strong linear correlation ($r = 0.89$) between the percentage of calcareous foraminifera and the planktonic-to-benthic ratio (Table 5). This correlation seems to support a relation between test composition among benthic foraminifera analyzed in this study and an environmental factor that independently affects also the abundances of planktonic foraminifera preserved in the sediment. In the central PIB, *i.e.* in relatively open water, planktonic-to-benthic ratios may reflect differences in dissolution and/or surface productivity (*e.g.* Berger and Diester-Haass 1988). Considering the rather narrow geographic range and assuming similar ages for the majority of the core tops (excluding the four suspect sites KC14, KC16, KC20, and KC23), large productivity differences between the sites analyzed in this study is rather unlikely. Moreover, fragmentation and corrosion of both benthic and planktonic foraminifera tests is apparent, pointing to dissolution within the water column and/or sediment as the major factor responsible for changes in percentages of calcareous foraminifera and plankton-to-benthos ratios (Fig. 12).

Increasing carbonate dissolution with water depth is closely related to the CCD, the depth at which calcium carbonate is dissolved as fast as it falls from above. Kellogg and Kellogg (1987) suggested it is situated in Amundsen Sea as between 300 and 500 mwd. The results of the present study, notably the significant drop in percentage of calcareous tests along with plankton-to-benthos ratio values across roughly 700 mwd (Fig. 12) as well as changes within benthic foraminiferal assemblages discussed in previous section, suggest that the CCD is slightly deeper. However, it should be kept in mind that foraminifera from the core tops do not represent modern assemblages, and so the CCD may have a different position at present. Infact, the location of the CCD at 300–500 mwd, suggested by Kellogg and Kellogg (1987), corresponds closely with the strong gradient in water temperature and salinity in PIB between 200 and 600 mwd (Jacobs *et al.* 2011, 2012). Below that depths, the relatively warm CDW dominates. This water mass influences practically all sites sampled during the present study. CDW is of mixed origin and includes a significant component of aged waters originating from the North Atlantic (Orsi *et al.* 1999). The corrosive nature of this water mass is apparent not only from the present observations, but also from the general scarcity of carbonates throughout PIB Holocene deposits (Lowe and Anderson 2002; Kirshner *et al.* 2012).

Similarly, Ishman and Domack (1994), who reported clear changes in foraminiferal assemblages along the margin of Antarctic Peninsula, suggested that the water mass distribution was the key environmental factor controlling benthic foraminiferal assemblages. The most south-westerly part of their study area was influenced by CDW and it was characterized by the presence of *Bulimina aculeata*, a calcareous benthic foraminifer that is also present in almost all core tops from PIB (Appendices 1 and 2). In the present study, *B. aculeata* is also an important accessory species for the calcareous *A. earlandi* FA of the > 125 μm dataset (Table 3A). This, supports the use of abundant *B. aculeata* as an index species for CDW influence.

Faunal comparison with other Antarctic regions. — As mentioned in the Introduction, numerous foraminiferal studies have been conducted in two other areas of West Antarctica: Ross Sea and South Shetlands. These offer an opportunity to compare foraminiferal assemblages from different regions of West Antarctica. A literature-based faunal comparison has its weaknesses. It may be biased by geographical and bathymetric range or by different habitats analyzed in particular studies, as well as taxonomic approaches of various authors. Not much can be done about the earlier, but the latest may be addressed by analyzing only these studies with good illustrations, allowing verification of taxonomic assignments. Following this criterion, the assemblages from PIB are compared with foraminifera from Deception Island (Finger and Lipps 1981) and Admiralty Bay of King George Island (Majewski 2005, 2010; Majewski *et al.* 2007), both located within South Shetland Islands, as well as from McMurdo Sound (Ward 1984; Gooday *et al.* 1996) and Terra Nova Bay (Violanti 1996) within Ross Sea.

Detailed results of this comparison are shown in Appendix 3. Among all species identified in PIB in this study, 54% were also reported from the South Shetlands and 59% from Ross Sea. Higher similarity with the Ross Sea fauna was also noted among the 32 species used for statistical analyses, see Tables 3A and 4A, showing 55% and 64% of species shared between PIB on one side, and South Shetlands and Ross Sea, respectively, on the other. This closer relationship of foraminiferal assemblages from PIB with the Ross Sea maybe partly due to the fact that the studies from South Shetlands explored predominantly water-depths shallower than those from the recent study, while surveys from Ross Sea either reached greater water-depths (Ward 1984; Violanti 1996) or investigated assemblages from shallow-water depths but showing clear deep-water characteristics (Gooday *et al.* 1996). Despite this bathymetric issue, it appears that the lower similarity of the PIB foraminifera with assemblages from South Shetlands may be a reality, as the latter is the warmest region of West Antarctica, significantly affected by strong cyclonic weather systems coming across the Drake Passage (King *et al.* 2003). It this respect South Shetlands differ significantly from both PIB and Ross Sea.

The comparison of the foraminiferal assemblages from PIB with assemblages described by Igarashi *et al.* (2001) from Lützow-Holm Bay, on the other side of the continent in East Antarctica, reveals even more intriguing results. Among all species reported in the present study, 62% were also recognized in Lützow-Holm Bay; among the 32 most important species, as many as 76% were also noted in that distant area. The corresponding numbers for the Ross Sea are 59% (all species) and 64% (important species). Even if this difference may be an artifact resulting from the more detailed survey of Igarashi *et al.* (2001), which included fossil (Holocene) as well as modern assemblages, it still shows that foraminiferal faunas may be quite similar throughout Antarctic shelf, reflecting comparable environmental conditions (*e.g.* similar water masses, near-glacial settings) at distant locations.

PIB in Amundsen Sea and Lützow-Holm Bay in East Antarctica could provide a good example of such environmentally-based faunal similarities around the Antarctic continent. Both areas share surprisingly similar benthic foraminiferal assemblages, and in both cases CDW intrusions seem to play an important role in shaping their present day environments (Igarashi *et al.* 2001; Kirshner *et al.* 2012). Thus, species that are well adapted to a wide range of Antarctic habitats may show supra-regional, circum-Antarctic distributions, the distribution pattern that has been already suggested for some benthic foraminiferal species around Antarctica (Mikhalevich 2004).

Conclusions

Although the benthic foraminiferal assemblages from Pine Island Bay and nearby Ferrero Bay show only moderate variability, they exhibit strong decrease in calcareous forms with increasing water depth across ~700 mwd. There were overall similarities in species composition and diversity across a rather narrow bathymetrical range of sampling (mainly 550–900 mwd) and under influence of relatively warm Circumpolar Deep Water. The abundant presence of *Bulimina aculeata* appears to reflect the influence of this water mass, for which it is considered to be the index species. The water-depth gradient in assemblage composition is interpreted to result from increasing dissolution of carbon carbonate with increasing depth, thus favoring agglutinated forms at deeper sites. Some irregularities in that gradient are most likely due to different ages of the analysed core tops.

In total, 93 benthic species, belonging to 71 genera, were identified. There are more species in common between the study sites and the Ross Sea than assemblages from the South Shetland Islands. The fact that fewer species are shared with the later area seems to be due to the significantly warmer climate in South Shetlands than in the Ross and Amundsen seas. Even more species are common to assemblages in Pine Island Bay and Lützow-Holm Bay in East Antarctica, which is much more distant than both the Ross Sea and South Shetland area, but is also influenced by Circumpolar Deep Water. This suggests that environmental characteristics play a more important role in benthic foraminiferal distribution across Antarctica than geography and that some taxa that are especially well adapted to polar conditions show wide, circum-Antarctic distributions.

Acknowledgements. — The sampling in PIB during the OSO0910 Expedition was possible thanks to collaboration between the US National Science Foundation (NSF), the Swedish Polar Research Secretariat, and the Swedish Research Council. I would like to thank the captain and crew of the icebreaker *Oden*, as well as all fellow researchers onboard for this great research opportunity. I am especially grateful to John B. Anderson, who invited me to join this project, supported by NSF grant ANT-0837925. I would like to thank two anonymous reviewers for their valuable comments.

References

BERGER W.H. and DIESTER-HAASS L. 1988. Paleoproductivity: The benthic/planktonic ratio in foraminifera as a productivity index. *Marine Geology* 81: 15–25.

BERNHARD J.M. 1987. Foraminiferal biotopes in Explorers Cove, McMurdo Sound, Antarctica. *Journal of Foraminiferal Research* 17: 286–297.

BRÖNNIMANN P. and WHITTAKER J.E. 1988. *The Trochamminacea of the Discovery Reports*. British Museum of Natural History, London: 152 pp.

CORLISS B.H. 1979. Taxonomy of Recent deep-sea benthonic foraminifera from the southeast Indian Ocean. *Micropaleontology* 25: 1–19.

FILLON R.H. 1974. Late Cenozoic foraminiferal paleoecology of the Ross Sea, Antarctica. *Micropaleontology* 20: 129–151.

FINGER K.L. and LIPPS J.H. 1981. Foraminiferal decimation and repopulation in an active volcanic caldera, Deception Island, Antarctica. *Micropaleonthology* 27: 111–139.

GOODAY A.J., BOWSER S.S. and BERNHARD J.M. 1996. Benthic foraminiferal assemblages in Explorers Cove, Antarctica: A shallow-water site with deep-sea characteristics. *Progress in Oceanography* 37: 117–166.

GRIFFITHS H.J. 2010. Antarctic marine biodiversity – What do we know about the distribution of life in the Southern Ocean? *PLoS ONE* 5: e11683.

IGARASHI A., NUMANAMI H., TSUCHIYA Y. and FUKUCHI M. 2001. Bathymetric distribution of fossil foraminifera within marine sediment cores from the eastern part of Lützow-Holm Bay, East Antarctica, and its paleoceanographic implications. *Marine Micropaleontology* 42: 125–162.

ISHMAN S.E. and DOMACK E.W. 1994. Oceanographic controls on benthic foraminifers from the Bellingshausen margin of the Antarctic Peninsula. *Marine Micropaleontology* 24: 119–155.

JACOBS S.S., JENKINS A., GIULIVI C.F. and DUTRIEUX P. 2011. Stronger ocean circulation and increased melting under Pine Island Glacier ice shelf. *Nature Geoscience* 4: 519–523.

JACOBS S.S., JENKINS A., HELLMER H., GIULIVI C., NITSCHE F., HUBER B. and GUERRERO R. 2012. The Amundsen Sea and the Antarctic Ice Sheet. *Oceanography* 25: 154–163.

JAKOBSSON M., ANDERSON J.B., NITSCHE F., DOWDESWELL J.A., GYLLENCREUTZ R., KIRCHNER N., MOHAMMAD R., O'REGAN M, ALLEY R.B., ANANDAKRISHNAN S., ERIKSSON B., KIRSHNER A., FERNANDEZ R., STOLLDORF T., MINZONI R. and MAJEWSKI W. 2011. Geological record of ice shelf break-up and grounding line retreat, Pine Island Bay, West Antarctica. *Geology* 39: 691–694.

KELLOGG D.E. and KELLOGG T.B. 1987. Microfossil distribution in modern Amundsen Sea sediments. *Marine Micropaleontology* 12: 203–222.

KING J.C., TURNER J., MARSHALL G.J., CONNOLLEY W.M. and LACHLAN-COPE T.A. 2003. Antarctic Peninsula climate variability and its causes as revealed by instrumental records. *Antarctic Research Series* 79: 17–30.

KIRSHNER A.E., ANDERSON J.B., JAKOBSSON M., O'REGAN M., MAJEWSKI W. and NITSCHE F.O. 2012. Post-LGM deglaciation in Pine Island Bay, West Antarctica. *Quaternary Science Reviews* 38: 11–26.

LOEBLICH A.R. and TAPPAN H. 1987. *Foraminiferal Genera and their Classification*. Van Nostrand Reinhold Company, New York: 970 pp.

LOWE A.L. and ANDERSON J.B. 2002. Reconstruction of the West Antarctic Ice Sheet in Pine Island Bay during the last glacial maximum and its subsequent retreat history. *Quaternary Science Reviews* 21: 1879–1897.

MACKENSEN A., GROBE H., KUHN G. and FÜTTERER D.K. 1990. Benthic foraminiferal assemblages from the eastern Weddell Sea between 68 and 73°S: Distribution, ecology and fossilization potential. *Marine Micropaleontology* 16: 241–283.

MAJEWSKI W. 2005. Benthic foraminiferal communities: distribution and ecology in Admiralty Bay, King George Island, West Antarctica. *Polish Polar Research* 26: 159–214.

MAJEWSKI W. 2010. Benthic foraminifera from West Antarctic fiord environments: An overview. *Polish Polar Research* 31: 61–82.

MAJEWSKI W. and PAWLOWSKI J. 2010. Morphologic and molecular diversity of the foraminiferal genus *Globocassidulina* in Admiralty Bay, West Antarctica. *Antarctic Science* 22: 271–281.

MAJEWSKI W., LECROQ B., SINNIGER F. and PAWŁOWSKI J. 2007. Monothalamous foraminifera from Admiralty Bay, King George Island, West Antarctica. *Polish Polar Research* 28: 187–210.

MAKSYM T., STAMMERJOHN S.E., ACKLEY S. and MASSOM R. 2012. Antarctic sea ice – A polar opposite? *Oceanography* 25: 140–151.

MALMGREN B.A. and HAQ B.U. 1982, Assessment of quantitative techniques in paleobiogeography. *Marine Micropaleontology* 7: 213–236.

MAYER M. 2000. Zur Ökologie der Benthos-Foraminiferen der Potter Cove (King George Island, Antarktis). *Berichte zur Polarforschung* 353: 1–126.

MEAD G.A. 1985. Recent benthic foraminifera in the Polar Front region of the southwest Atlantic. *Micropaleontology* 31: 221–248.

MIKHALEVICH V.I. 2004. The general aspects of the distribution of Antarctic foraminifera. *Micropaleontology* 50: 179–194.

NITSCHE F.O., JACOBS S.S., LARTER R.D. and GOHL K. 2007. Bathymetry of the Amundsen Sea continental shelf: implications for geology, oceanography, and glaciology. *Geochemistry, Geophysics, Geosystems* 8: Q10009.

ORSI A.H., JOHNSON G.C. and BULLISTER J.L. 1999. Circulation, mixing and production of Antarctic bottom water. *Progress in Oceanography* 43: 55–109.

OSTERMAN L.E. and KELLOGG T.B. 1979. Recent benthic foraminiferal distribution from the Ross Sea, Antarctica: relation to ecologic and oceanographic conditions. *Journal of Foraminiferal Research* 9: 250–269.

PFLUM C.E. 1966. The distribution of the foraminifera of the eastern Ross Sea, Amundsen Sea and Bellingshausen Sea, Antarctica. *Bulletins of American Paleontology* 50 (226): 151–209.

RIGNOT E. and THOMAS R.H. 2002. Mass balance of polar ice sheets. *Science* 297: 1502–1506.

RIGNOT E., BAMBER J.L., VAN DEN BROEKE M.R., DAVIS C., LI Y.H., VAN DE BERG W.J. and VAN MEIJGAARD E. 2008. Recent Antarctic ice mass loss from radar interferometry and regional climate modelling. *Nature Geoscience* 1: 106–110.

RODRIGUES A.R., MALUF J.C.C., BRAGA E.D.S. and EICHLER B.B. 2010. Recent benthic foraminiferal distribution and related environmental factors in Ezcurra Inlet, King George Island, Antarctica. *Antarctic Science* 22: 343–360.

SILVA K.A., CORLISS B.H., RATHBURN A.E. and THUNELL R.C. 1996. Seasonality of living benthic foraminifera from the San Pedro Basin, California Borderland. *Journal of Foraminiferal Research* 26: 71–93.

THOMA M., JENKINS A., HOLLAND D. and JACOBS S. 2008. Modelling Circumpolar Deep Water intrusions on the Amundsen Sea continental shelf, Antarctica. *Geophysical Research Letters* 35: L18602.

VIOLANTI D. 1996. Taxonomy and distribution of recent benthic foraminifers from Terra Nova Bay (Ross Sea, Antarctica), Oceanographic Campaign 1987/1988. *Palaeontographia Italica* 83: 25–71.

WALKER D.P., BRANDON M.A., JENKINS A., ALLEN J.T., DOWDESWELL J.A. and EVANS J. 2007. Oceanic heat transport onto the Amundsen Sea shelf through a submarine glacial trough. *Geophysical Research Letters* 34: L02602.

WARD B.L. 1984. *Distribution of modern benthic foraminifera of McMurdo Sound, Antarctica*. M.Sc. Thesis. Victoria University, Wellington: 211 pp. (unpublished).

WARD B.L., BARRETT P.J. and VELLA P. 1987. Distribution and ecology of benthic foraminifera in McMurdo Sound, Antarctica. *Palaeogeography, Palaeoclimatology, Palaeoecology* 58: 139–153.

WIESNER H. 1931. Die Foraminiferen der Deutschen Südpolar Expedition 1901–1903. *Deutschen Südpolar Expedition* 20: 53–165.

Received 17 December 2012
Accepted 19 April 2013

Appendix 1

Foraminiferal counts from the > 125 µm grain-size fraction (> 125 µm dataset).

Core ID	KC04	KC06	KC07	KC09	KC10	KC11	KC13	KC14	KC15	KC16	KC17	KC18	KC19	KC20	KC1	KC22	KC23	KC24	KC25	KC26	KC27
Fraction of sample picked	0.25	0.125	0.068	0.011	0.031	0.125	0.174	0.133	1	0.063	0.2	0.115	0.078	0.179	0.0313	0.047	0.089	0.063	0.317	0.068	0.052
Bathysiphon argenteus	1					1	1							1		3					1
Bathysiphon flexilis	1		1																		
Rhabdammina spp.	41	40	32	5	4	25	40	39	4	13	22	23	22	29	22	18	42	48	30	31	29
?*Hippocrepinella* sp.	1						1		5	1	4						1	2	1	1	1
Hyperammina fragilis	1		1		1	1		1	1	2			3			1		2			
Pelosina bicaudata		1		1				1		1	1	1		1	1		1		1		3
Psammosphaera spp.							1		4		3		1		5	1	4	3	4	2	2
Saccammina tubulata			1				1				2		1		1	1	1		1		
?*Lagenammina* sp.							3					3									
Ammodiscus incertus						1		1				1						1			
Reophax subdentaliniformis	4	1	5			2	2	7	1	5	2		1	4	5	3	2	1			
Reophax scorpiurus	2	2		1			1	7		4	4		7	1			3	1	1	3	3
Reophax cf. *R. spiculifer*	7	1	6		1	6	3	4	2	6	12	3	8	3	3	4	3	8	6	7	5
Pseudonodosinella nodulosa	3	2	1				1	1	3								4			1	1
Nodulina cf. *N. dentaliniformis*										8											
Hormosinella spp.	14	4	10	5	1	23	19	8	14	8	11	18	19	2	7	6	9	18	30	8	2
Cystammina argentea							1			1		1							1		
Miliammina arenacea	7		5	2	1	2	2	6	5	10	4	15	19	11	3	2	8	15	11	4	1
Adercotryma glomerata	2		4	1		7	9	3	4	8	8	11	8	3	8	7	7	6	8	11	3
Pseudobolivina antarctica	2	2	5			1	1			4	1	2	2	1		4	5	1			1
Eggerella nitens	1	3	3	2	1		1	1							3		2	3		1	
Eggerella bradyi		4	1	1				2	2	2		3	2					2	3		1
Verneuilina minuta			1			2								2			1				
Spiroplectammina biformis	10	6	2		1	10	1	3	2	3	1	1	5	8	2	6	5	2	1	7	3
Cyclammina trullissata	2																				
Cyclammina pusilla	7	10	3		1	6	3	2						5			7	1		3	1
Labrospira wiesneri	2	1	1			1		1		1		2	1	4	1	1			1	1	3
Labrospira jeffreysii	1	8	1	4	1			4	1	7	2		2	5		2	5			1	5
Labrospira sp.					1	2	1	1	3	8	3	2		1						1	
Eratidus foliaceus	4		1			1	6		1		5	18	2	14		1	1	6	8	3	4
Paratrochammina lepida			0						2	3	1									1	
Recurvoides contortus	2								9	1	9	3	3					2	5	1	
Atlantinella atlantica			1			1				1						1					

Core ID	KC04	KC06	KC07	KC09	KC10	KC11	KC13	KC14	KC15	KC16	KC17	KC18	KC19	KC20	KC1	KC22	KC23	KC24	KC25	KC26	KC27
Fraction of sample picked	0.25	0.125	0.068	0.011	0.031	0.125	0.174	0.133	1	0.063	0.2	0.115	0.078	0.179	0.0313	0.047	0.089	0.063	0.317	0.068	0.052
Polystomammina falklandica				1					1		1			1			1			1	
Portatrochammina spp.	1	11	1	5		10	6	9	2	24	25	19	21		13	12	18	19	14	4	13
Portatrochammina antarctica	2	4		1		4		6		6	10		2	3				1	4	2	
Portatrochammina cf. *P. antarctica*									1		1										
Portatrochammina bipolaris										3	1	1									
Portatrochammina cf. *P. quadricamerata*				3			1	2		1		1			3			3	2		
Alterammina alterans	12	11	13	1		31	24	17	16		14	10	16	25	3	8	4	13	24	9	5
Other agglutinated	1			4		4	2	3	2	18	2	4	2			1	1	1	1	1	
Triloculinella spp.	2		2		1	1	2			1	1		2		3			1			
Lenticulina angulata		1			1	1										1					
Pyrgo elongata									3		1										
Various lagenidae	2	3		1	2	2						1				1					
Hyalinonetrion sp.		2																			
Bolivinellina pseudopunctata	1		1				2														1
Bolivinellina earlandi										3											
Bolivina cf. *B. spinescens*	2		1		4										1	1		1			1
Bulimina aculeata	14	30	17	11	44	6	2	3			1		2	2	15	16	2		1	15	15
Stainforthia concava	2		1									1	1			1					
Angulogerina earlandi	15	93	10	46	75	2	2	16				5	3	4	27	23	13	3	2	14	27
Pullenia salisburyi	1		1								1			1	1	2		1			
Astrononion antarcticum			1	1																	
Astrononion echolsi		1		1	4			1	1	5	2			1		2					1
Nonionella iridea	1	1		9	5	1	2					1				3				1	
Cassidulina carinata			1	3	8										1						1
Globocassidulina spp.	7	10	13	7	18	4	9	5	4	2	2	8	1	2	7	7		2	1	7	8
Rosalina globularis				1											1						
Oridorsalis sidebottomi		3							2							1				2	
Gyroidina sp.			2	4	1	1														1	
Cibicides refulgens	1			1	4															1	1
Lobatula lobatula				15	8																
Ioanella tumidula		8	4	5	3	1	1								5	3	2			3	3
Epistominella spp.		2	6	21	11	5	6					2	2		12	11	1	1		6	4
Other calcareous benthics	2		1	1		1	1								3						1
Neogloboquadrina pachyderma	66	206	140	326	747	18	31	22		3	4	12	6	3	87	99	2	8	11	87	80

Appendix 2

Foraminiferal counts from the 63–125 µm grain-size fraction. These data combined with the results from the > 125 µm fraction contributed to generate the total assemblages (> 63 µm dataset).

Core ID	KC04	KC06	KC07	KC09	KC10	KC11	KC13	KC14	KC15	KC16	KC17	KC18	KC19	KC20	KC21	KC22	KC23	KC24	KC25	KC26	KC27
Fraction of sample picked	0.021	0.067	0.027	0.003	0.004	0.038	0.075	0.034	1	0.031	0.156	0.1	0.031	0.125	0.008	0.016	0.048	0.05	0.175	0.019	0.023
Bathysiphon argenteus						1		2	1	1		1	1	1		2				3	
Bathysiphon flexilis			1	1		3	1	1													
Rhabdammina spp.	1		5	1			3	6	1	3	2	2	4	7	1	2	7	13	7	6	
?*Hippocrepinella* sp.									1		3										
Hyperammina fragilis														2							
Pelosina bicaudata																					
Psammosphaera spp.									3		1										
Saccammina tubulata																					
?*Lagenammina* sp.																					
Ammodiscus incertus													2	1							
Reophax subdentaliniformis	1					1	1			5		1		1	1	1	1	1		1	
Reophax scorpiurus			1					1												1	2
Reophax cf. *R. spiculifer*			1			1	1	2	5		5		2		1			3			
Pseudonodosinella nodulosa																					
Nodulina cf. *N. dentaliniformis*																					
Hormosinella spp.			1				1		3	6	2	4	4	1				1			
Cystammina argentea						2	1	1	5	2	5	3	7	3		1		5	4	4	
Miliammina arenacea	2		1				3	5	1	5	2	10	8	7			3	12	2	2	1
Adercotryma glomerata	15	3	6	1		24	25	14	13	13	21	27	38	23	16	12	26	23	20	19	15
Pseudobolivina antarctica	7	7	3	2		28	31	21	4	24	8	24	45	20	15	8	23	19	19	14	6
Eggerella nitens																1					
Eggerella bradyi				1																	
Verneuilina minuta				1										1			1				
Spiroplectammina biformis	11	7	8			8	6	21	13	16	13	6	5	25	13	8	23	20	3	10	13
Cyclammina trullissata																					
Cyclammina pusilla																					
Labrospira wiesneri	4			1		4		1		1	3			6			7			1	3
Labrospira jeffreysii	2																1				
Labrospira sp.									4	4	2										1
Eratidus foliaceus											2	1	2				1	1	1		
Paratrochammina lepida		1		5		1		1	1	8	9		1	1	1		3	2			3
Recurvoides contortus																					

Core ID	KC04	KC06	KC07	KC09	KC10	KC11	KC13	KC14	KC15	KC16	KC17	KC18	KC19	KC20	KC21	KC22	KC23	KC24	KC25	KC26	KC27
Fraction of sample picked	0.021	0.067	0.027	0.003	0.004	0.038	0.075	0.034	1	0.031	0.156	0.1	0.031	0.125	0.008	0.016	0.048	0.05	0.175	0.019	0.023
Atlantinella atlantica																					
Polystomammina falklandica								1	1		8	1	1	2		2	2	2	1	1	
Portatrochammina spp.	17	4	4	2	0	10	16	33	33	55	50	35	22	22	15	9	25	32	44	14	17
Alteramina alterans			2			3	2	5	3		8	4	3	3		4	2	6	4		
Other agglutinated		1		2		2		2	2	1		2	2				2				2
Triloculinella spp.	1	1																			
Lenticulina angulata					1		1														
Pyrgo elongata																					
Various lagenidae										1	1										
Hyalinonetrion spp.																					
Bolivinellina pseudopunctata	1	1					2			1			1		2			1			
Bolivinellina earlandi									2	5	1								1		
Bolivina cf. *B. spinescens*																					
Bulimina aculeata	1	4	5	3	8		1							1	2	8	1		1	1	6
Stainforthia concava		2	2					1							2					1	
Angulogerina earlandi		2		2	1	1		1				1		1		1					
Pullenia salisburyi																					
Astrononion antarcticum														1							
Astrononion echolsi				2					2	2	1										
Nonionella iridea		2	2	5	2			2	1			2	4		2	3			6	1	3
Cassidulina carinata																					
Globocassidulina spp.	4	3	11	5	8	5	1	4		3	1	5	2	2	2	7			5	3	6
Rosalina globularis																					
Oridorsalis sidebottomi																					
Gyroidina sp.																					
Cibicides refulgens	2																			1	2
Lobatula lobatula				5	6	1															
Ioanella tumidula	13	14	6	13	11	7	4	6						6	7	11	4	3		5	9
Epistominella spp.	102	99	93	102	110	48	61	23	9	3	3	31	22	13	85	75	18	12	53	66	68
Other calcareous benthics				3	3				2				1			1					
Neogloboquadrina pachyderma				18	6	2	3									3		1			1

Appendix 3

Taxonomical list. Numbers in parentheses indicate the same taxa reported from other areas of West Antarctica, *i.e.* South Shetland Islands: 1 (Deception Island; Finger and Lipps 1981), 2 (Admiralty Bay, King George Island; Majewski 2005, 2010; Majewski *et al.* 2007) and Ross Sea: 3 (McMurdo Sound; Ward 1984; Gooday *et al.* 1996), 4 (Terra Nova Bay; Violanti 1996), as well as from East Antarctica 5 (Lützow-Holm Bay; Igarashi *et al.* 2001).

Adercotryma glomerata (Brady, 1878); Fig. 4.4 (1, 2, 3, 5).
Alterammina alterans (Earland, 1934); Figs 7.4–5 (3, 4, 5).
Ammodiscus incertus (d'Orbigny, 1839); Fig. 3.4 (1, 2, 4, 5).
Angulogerina earlandi Parr, 1950; Figs 9.13–14 (2, 3, 4, 5).
?*Astrammina* sp.; Fig. 2.12 (2, 4, 5).
Astrononion antarcticum Parr, 1950; Figs 10.5–6 (1, 2, 3, 4, 5).
Astrononion echolsi Kennet, 1967; Fig. 10.7 (1, 2, 3, 4, 5).
Atlantinella atlantica (Parker, 1952); Fig. 5.10 (2, 5).
Bathysiphon argenteus Heron-Allen *et* Earland, 1913; Figs 2.1–2 (2, 3, 4).
Bathysiphon flexilis Höglund, 1947; Fig. 2.3 (1, 2).
?*Botuloides* sp.; Fig. 9.1 (3).
Bolivina cf. *B. spinescens* Cushman, 1911; Figs 9.6–7.
Bolivinellina earlandi (Parr, 1950); Fig. 9.4 (1, 5).
Bolivinellina pseudopunctata (Höglund, 1947); Fig. 9.3 (1, 2, 3, 4).
Bulimina aculeata d'Orbigny, 1826; Figs 9.8–9 (1, 5).
Cassidulina carinata Silvestri, 1896; Fig. 10.10 (5?).
Cibicides refulgens de Montfort, 1808; Fig. 11.4 (1, 2, 4, 5).
Cornuspira involvens (Reuss, 1850); Fig. 9.5 (1, 2, 3).
Cyclammina pusilla Brady, 1884; Fig. 4.13.
Cyclammina trullissata (Brady, 1879); Fig. 4.12.
Cystammina argentea Earland, 1934; Fig. 4.1.
Eggerella bradyi (Cushman, 1911); Fig. 4.9.
Eggerella nitens (Wiesner, 1931); Figs 4.7–8 (5).
Ehrenbergina glabra Heron-Allen *et* Earland, 1922; Fig. 10.13 (3, 4, 5).
Epistominella spp.; Figs 11.8–9 (1, 2, 3, 4, 5).
Eratidus foliaceus (Brady, 1881); Figs 5.3–4 (5?).
Exsculptina sp.; Fig. 8.1.
Favulina hexagona (Williamson, 1848); Fig. 8.3 (3, 4).
Favulina scalariformis (Williamson, 1848); Fig. 8.4.
Galwayella trigonoeliptica (Balkwill *et* Millett, 1884); Fig. 8.8.
Globocassidulina spp.; Figs 10.11–12 (1, 2, 3, 4, 5). All specimens are small and medium in size, at the most up to 500 μm in length. None shows double aperture, typical for adult *G. biora*, nor strongly bifurcated typical for *G. rosensis*. The smallest specimens show single, perpendicular or oblique to the basal suture of the last chamber, larger curved, sometimes to the point of initial bifurcation. According to recent molecular study, individuals of differently shaped apertures in different ontogenetic stages may belong to a single species (Majewski and Pawlowski 2010) for that reason precise classification of minute, often immature specimens based solely on morphology is problematic at this point.
Glomospira gordialis (Jones *et* Parker, 1860); Fig. 3.3 (1, 2, 3, 4, 5).
Gyroidina sp.; Fig. 11.3 (5). It closely resembles specimens of *Gyroidinoides* from South Atlantic illustrated by Mead (1985; plate 5, figs 1–7), *Alabaminella weddelliensis* (Earland 1936) pictured by Igarashi *et al.* (2001; plate 11, fig. 10), and that of *Gyroidinoides soldanii*

(d'Orbigny 1826) in Corlis (1979; plate 5, figs 4–6) but in all cases it differs from the holotypes.

?*Hippocrepinella* sp.; Fig. 2.8 (1, 2, 3).

Hormosinella spp.; Figs 3.15–16 (1, 2, 3, 4, 5).

Hyalinonetrion sp.; Fig. 8.12 (2, 3, 5).

Hyperammina fragilis Höglund, 1947; Fig. 2.9 (3).

Ioanella tumidula (Brady, 1884); Figs 11.6–7 (5).

Labrospira jeffreysii (Williamson, 1858); Fig. 5.5 (1, 2, 3, 4, 5).

Labrospira wiesneri Parr, 1950; Fig. 5.6 (2, 3, 5).

Labrospira sp.; Figs 5.1–2.

Laevidentalina communis (d'Orbigny, 1826); Fig. 9.2 (2, 3, 4).

Lagena cf. *L. texta* Wiesner, 1931; Fig. 8.5 (3).

Lagena sp.; Fig. 8.2 (5). It shows some similarities with *L. subacuticosta* Parr, 1950 in overall shape, ornamentation, and shows signs of attachment of second individual at the base of the illustrated specimen, similarly as on specimen 210 on plate 18 of Wiesner (1931). On the other hand, lacking the collar of shell material around the base of the apertural neck and having very broad costae suggests its similarity with *Lagena* sp. 4 and *Lagena* sp. 5 illustrated by Igarashi *et al.* (2001) from East Antarctica.

Lagenammina sp.; Fig. 2.19. Its finely agglutinated wall differs from coarsely agglutinated *Lagenammina* species common throughout Antarctica (*e.g.* Ward 1984; Igarashi *et al.* 2001; Majewski 2005).

Lenticulina angulata (Reuss, 1851); Figs 10.1–2 (3, 5).

Lobatula lobatula (Walker *et* Jacob, 1798); Fig. 11.5 (1, 2, 3, 4, 5).

Miliammina arenacea (Chapman, 1916); Fig. 4.2 (1, 2, 3, 4, 5).

Miliammina lata Heron-Allen *et* Earland, 1930; Fig. 4.3 (2, 3, 4, 5).

Nodulina cf. *N. dentaliniformis* (Brady, 1884); Fig. 3.13 (1, 2, 3, 4). Differs from the holotype described by Brady by more elongated chambers.

Nonionella iridea Herron-Allen *et* Earland, 1932; Figs 10.8–9 (1, 2, 3, 4, 5).

?*Oolina* sp.; Fig. 8.10 (2, 4).

Oridorsalis sidebottomi (Earland, 1934); Fig. 11.2 (5).

Parafissurina sp.; Fig. 8.6 (5).

Parafissurina ventricosa (Silvestri, 1904); Fig. 8.7 (2, 3, 5).

Paratrochammina (*Lepidoparatrochammina*) *lepida* Brönnimann *et* Whittaker, 1988; Figs 5.7–8 (2, 3, 4, 5).

Pelosina bicaudata (Parr, 1950); Fig. 2.10 (2, 3).

Polystomammina falklandica Brönnimann *et* Whittaker, 1988; Fig. 6.1. With chamber shape and arrangement it resembles *Deuterammina* (*Deuterammina*) *grisea* (Earland, 1934) but it appears to lack a primary interiomarginal aperture, characteristic for this genus (Brönnimann and Whittaker 1988).

Portatrochammina antarctica Parr, 1950; Figs 6.3–4 (1, 2, 3, 4, 5).

Portatrochammina cf. *P. antarctica* Parr, 1950; Figs 6.6–7. This taxon includes relatively large specimens, which major characteristics are these of *P. antarctica* Parr, 1950; however, its wall is composed in large of barite granules, which in early chambers may be especially abundant.

Portatrochammina bipolaris Brönnimann *et* Whittaker, 1980; Fig. 6.5 (2, 3, 4, 5).

Portatrochammina cf. *P. quadricamerata* (Echols, 1971); Fig. 6.2 (4, 5).

Portatrochammina spp. (1, 2, 3, 4, 5) includes *P. antarctica*, *P. bipolaris*, and *Portatrochammina* cf. *P. quadricamerata* (all listed above and shown on Figs 6.3–7) and probably a number of other species, which are impossible to distinguish in immature, minute forms. For this reason, abundances of this genus are treated cumulatively for the statistical analysis. Immature specimens shown on Figs 7.1–2 include specimens with four chambers in the final whorl and simple, interiomarginal, or areal aperture that may be surrounded by thin rim.

Procerolagena gracilis (Williamson, 1848); Fig. 8.14 (2, 3).

Procerolagena meridionalis (Wiesner, 1931); Fig. 8.13 (3, 4, 5). Specimens from PIB are less densely ornamented than specimen pictured by Wiesner (1931).

Psammosphaera fusca Schulze, 1875; Fig. 2.15 (1, 2, 3, 4, 5).

Psammosphaera sp. 1; Fig. 2.13.

Psammosphaera sp. 2; Fig. 2.14.

Pseudobolivina antarctica Wiesner, 1931; Figs 4.5–6 (1, 2, 3, 4, 5).

Pseudonodosinella nodulosa (Brady, 1879); Fig. 3.11 (5).

Pseudonodosinella cf. *P. nodulosa* (Brady, 1879); Fig. 3.12.

Pseudotrochammina bullata (Höglund, 1947); Fig. 7.3 (3, 4).

?*Pseudothurammina* sp.; Fig. 3.1.

Pullenia salisburyi Stewart *et* Stewart, 1930; Figs 10.3–4 (5?).

Pygmaeoseistron hispidulum (Cushman, 1913); Fig. 8.11 (5).

Pyrgo elongata (d'Orbigny, 1826); Fig. 7.8 (1, 2, 3, 4, 5).

Quinqueloculina sp.; Fig. 7.6 (2). It shows similarity in chamber arrangement with *Quinqueloculina weaveri* from Majewski (2005; fig. 17.4), but chambers in specimens from PIB are not angular in cross section as in specimens from Admiralty Bay.

Recurvoides contortus Earland, 1934; Fig. 5.9 (1, 2, 3, 4, 5).

Reophax scorpiurus de Montfort, 1808; Figs 3.6–8 (1, 2, 3, 4, 5).

Reophax cf. *R. spiculifer* Brady, 1879; Fig. 3.10 (4, 5). Differs from the holotype described by Brady by having test walls built not entirely from sponge spicules.

Reophax subdentaliniformis Parr, 1950; Fig. 3.5 (1, 2, 4, 5).

Reophax sp.; Fig. 3.9.

?*Reophax* sp.; Fig. 3.14.

Rhabdammina spp.; Figs 2.4–7 (1, 2, 3, 4, 5).

Robertinoides sp.; Fig. 9.12 (4, 5).

Rosalina globularis d'Orbigny, 1826; Fig. 11.1 (1, 2, 3, 4, 5).

Saccammina tubulata Rhumbler, 1931; Figs 2.16–18.

Spiroplectammina biformis (Parker *et* Jones, 1865); Fig. 4.11 (1, 2, 3, 4, 5).

Stainforthia concava (Höglund, 1947); Figs 9.10–11 (2, 3, 4, 5).

Tholosina sp.; Fig. 3.2 (2?).

Thurammina albicans Brady, 1879; Fig. 2.11 (2, 3).

Triloculinella sp.; Fig. 7.7 (5). It resembles *Triloculina* aff. *tricarinata sensu* Parker, Jones *et* Brady, 1865 pictured by Igarashi *et al.* (2001), but unlike *Triloculina* it shows four chambers in the last whorl.

?*Vasicostella* sp.; Fig. 8.9 (5). It was classified by Igarashi *et al.* (2001) as *Vasicostella striatopunctata* (Parker *et* Jones, 1865), but it is quite different from *Lagena sulcata* var. *striatopunctata* originally described by Parker and Jones. On the other hand, it carries similarity in shape and ornamentation with *Lagena striatopunctata* var. *inaequalis* Sidebottom, 1912, but lacks strong punctuation of the costae.

Verneuilina minuta Wiesner, 1931; Fig. 4.10 (1, 2, 3, 5).